frontiers in Materials

REVIEW
published: 20 December 2019
doi: 10.3389/fmats.2019.00325

Research Progress of the Liquid-Phase Exfoliation and Stable Dispersion Mechanism and Method of Graphene

Liangchuan Li[1†], *Ming Zhou*[1*†], *Long Jin*[1*], *Lincong Liu*[1], *Youtang Mo*[1], *Xiao Li*[2], *Zhaoyou Mo*[3], *Zhenzhao Liu*[3], *Shengli You*[1] *and Hongwei Zhu*[4]

[1] School of Mechanical Engineering, Guangxi University of Science and Technology, Liuzhou, China, [2] Chengdu Carbon Co., Ltd., Chengdu, China, [3] Tsinglube Technologies Co., Ltd., Liuzhou, China, [4] State Key Laboratory of New Ceramics and Fine Processing, School of Materials Science and Engineering, Tsinghua University, Beijing, China

Graphene is a honeycomb hexagonal two-dimensional (2D) crystal nanomaterial with a thickness of only 0.334 nm. It has been widely used and studied because of its ultra-thin 2D nano-characteristics and excellent electrical, thermal, optical, and mechanical properties. With the continuous in-depth study of graphene, the liquid-phase dispersion of graphene has also achieved breakthroughs. This review summarizes the research progress of the liquid-phase exfoliation mechanism, exfoliation method, stable dispersion mechanism, and dispersion method of graphene in recent years. The research situations of the Hamaker constant theory in exfoliation mechanism and Hansen solubility coefficient theory in stable dispersion mechanism are mainly discussed. The shortcomings of the research are summarized and analyzes the graphene liquid phase dispersed in the important challenge in the future. The stable dispersion method of graphene is also summarized. In the future, the π-π interaction will be the most potential method for studying graphene stabilization.

Keywords: graphene, liquid-phase exfoliation, stable dispersion, Hamaker constant, Hansen solubility coefficient, π-π interaction

OPEN ACCESS

Edited by:
Antonio Di Bartolomeo, University of Salerno, Italy

Reviewed by:
Brigida Alfano, Italian National Agency for New Technologies, Energy and Sustainable Economic Development (ENEA), Italy
Mariano Palomba, Italian National Research Council, Italy

***Correspondence:**
Ming Zhou
zhoum03@mails.tsinghua.edu.cn
Long Jin
jlong1719@gmail.com

[†]*These authors have contributed equally to this work*

Specialty section:
This article was submitted to Thin Solid Films, a section of the journal Frontiers in Materials

Received: *03 July 2019*
Accepted: *27 November 2019*
Published: *20 December 2019*

Citation:
Li L, Zhou M, Jin L, Liu L, Mo Y, Li X, Mo Z, Liu Z, You S and Zhu H (2019) Research Progress of the Liquid-Phase Exfoliation and Stable Dispersion Mechanism and Method of Graphene. Front. Mater. 6:325. doi: 10.3389/fmats.2019.00325

INTRODUCTION

Materials are the basis and forerunner for the development of human society (Du, 2007; Wegst et al., 2015), and the birth of new materials is an important milestone of social progress. New materials technology of modern industries supports human civilization. Carbon materials are one of the richest resources on earth and play an important role in the history of human development (Cheng, 1998). After the discovery of fullerenes in 1985 and carbon nanotubes (CNTs) in 1991, the existence of materials with zero-dimensional (Fuller sphere), one-dimensional (1D) (CNTs), and three-dimensional (3D) (graphite) carbon has been confirmed by experiments (Cheng et al., 2006; Zhang, 2018). In 2004, Geim and Novoselov of Manchester University adopted the tape stripping method to prepare high-quality single-layer graphene for the first time (Novoselov et al., 2004), overturning the recognition that the finite temperature, classical thermal theory does not allow the perception of the existence of two-dimensional (2D) crystals (Xu et al., 2009). Graphene is a 2D nanomaterial composed of a single layer of carbon atoms and is closely mixed with sp^2 (Si and Samulski, 2008; Zhu et al., 2013). Its surface has a large area of π-π conjugated bond and has excellent electrical properties (at room temperature, electron

mobility: 15,000 $\frac{cm^2}{[V \cdot s]}$) (Allen et al., 2010; Green and Hersam, 2010; Brownson, 2013), thermal properties (thermal conductivity: 5,300 $\frac{W}{[m \cdot K]}$, which is 10 times higher than that of copper and aluminum) (Sadasivuni et al., 2014; Xu et al., 2016), mechanical properties (tensile strength: 130 GPa, which is 100 times that of steel) (Sadasivuni et al., 2014; Long et al., 2016), optical properties (single-layer transmittance: 97%, 2.3% for each additional layer absorbance) (Zhang et al., 2009; Cao and Guo, 2016), and a large specific surface area (2,630 m^2/g) (Kim et al., 2010; Zou et al., 2014). Given graphene's excellent 2D nano-features, the modification of SnO_2 with highly conductive 2D naphthalene diimide graphene can increase surface hydrophobicity and form van der Waals interaction between the surfactant and the organic–inorganic hybrid lead halide perovskite compounds. As a result, highly efficient perovskite solar cells with power conversion efficiency of 20.2% can be achieved with an improved fill factor of 82%, which could be mainly attributed to the augmented charge extraction and transport (Zhao X. J. et al., 2018). In anti-corrosion coating applications, graphene can block oxygen molecules and corrosion factors from penetrating into the coating substrate and improve the salt spray resistance of the coating by 20% and the antibacterial property by 50% (Gu et al., 2015, 2016; Wang et al., 2016; Zhao et al., 2017). As lithium-ion battery electrode materials, graphene and lithium iron phosphate are mixed, which increases the reversible specific capacity of the battery by 1.4 times (Cao et al., 2014; Uchaker and Cao, 2014). As a lubricating oil additive, the 2D layered structure of graphene has a friction coefficient reduced by up to 30% compared with ordinary lubricating oil through the interlayer slip effect (Liu L. L. et al., 2018; Liu et al., 2019). However, the van der Waals force between graphene sheets is prone to agglomeration (Li and Shi, 2014; Xie et al., 2014). As a result, it is neither lipophilic nor hydrophilic (Li et al., 2008), and it is difficult to uniformly disperse in various liquid media in practical applications (Vallés et al., 2008; Wan et al., 2013; Cui and Zhou, 2018). Obviously, the liquid-phase dispersion of graphene is the core problem that must be overcome in the experimental study of nanomaterials (Tang et al., 2009; Coletti et al., 2013; Wang and Chen, 2015; Sahoo and Ramaprabhu, 2017; Yu et al., 2018) to promote its industrial production (Yang K. et al., 2010; Secor et al., 2013; Wang and Chen, 2015; Fadavi et al., 2016; Huan-Yan et al., 2018).

Graphene liquid-phase dispersion can be divided into two parts: graphene exfoliation (because the degree of exfoliation of graphene determines its dispersion grade) and graphene stable dispersion. The exfoliation theory is the major discipline problem involving molecular inter-atomic forces, and its final goal is to overcome the graphene sheet interlayer van der Waals force and graphene layer interaction between functional groups. Blocking the adjacent layers of graphene to each other achieves monolayer of graphene. To quantify the graphene interlayer van der Waals force, researchers established the Hamaker constant (Diba et al., 2016) theory on the basis of intermolecular forces. The stable dispersion theory major discipline involved in the problem is the interface between the molecules of the solution theory. That is, an appropriate dispersant–solvent system that interacts with the graphene surface must be selected to improve the liquid medium interface properties and realize the uniform and stable dispersion of graphene. To cope with graphene matching an appropriate dispersant–solvent system, researchers studied the potential energy of the graphene surface and its relationship with the potential energy of the dispersant–solvent system, eventually believing the stability of the graphene dispersion and dispersant–solvent system of Hansen solubility coefficient (HSP) (Lim et al., 2014).

In this paper, the liquid-phase dispersion theory of graphene is reviewed from the aspects of liquid-phase exfoliation and stable dispersion. Firstly, aiming at overcoming the van der Waals force between graphene sheets, the progress of graphene liquid-phase exfoliation theory in recent years was summarized. The research results of the Hamaker constant theory were reviewed in each research group, and the advantages and disadvantages of the main exfoliation methods (e.g., ultrasonic degradation, mechanical exfoliation, and electrochemical exfoliation) were reviewed and analyzed. Then, in the mechanism of stable dispersion of graphene, the theory of the HSP was discussed, which was the basis for selecting a suitable dispersant–solvent system to interact with graphene. Finally, the research progress of stable dispersion methods of graphene was summarized, especially the π-π interaction in the stable dispersion methods of graphene.

LIQUID-PHASE EXFOLIATION OF GRAPHENE

Mechanism of Graphene Liquid-Phase Exfoliation

Currently, compared with the low-yield solid phase (Novoselov et al., 2004; Gao et al., 2018; Melios et al., 2018) (e.g., micromechanical exfoliation and epitaxial growth on SiC) method and the high-energy-consuming gas phase method (e.g., chemical vapor deposition) (Cai Z. Y. et al., 2018; Mao et al., 2018; Xia et al., 2018; Cheng et al., 2019), the liquid-phase exfoliation method has the advantages of higher processability, lower cost (Artur and Paolo, 2016), shorter preparation period, and larger-scale preparation (Artur and Paolo, 2014; Paton et al., 2014; Yang et al., 2015; Zhang et al., 2017). Liquid-phase exfoliation of graphene is a process in which graphite (or multilayer graphene) is converted into a single layer (or a few layers) of graphene by overcoming the van der Waals force between sheets (Allen et al., 2010). The van der Waals force between graphene sheets is mainly composed of Keesom interaction, Debye interaction, and dispersive force (Alecrim et al., 2015), where the dispersive force is the most important interaction force that constitutes the van der Waals force between atoms and molecules, and the intensity is generally less than the Coulomb force or hydrogen bonding (Israelachvili, 2011). With different exfoliation methods to overcome the van der Waals force between layers, the dispersant–solvent system enters the graphene sheet layer and interacts with its surface to achieve stable dispersion of the liquid phase (Fu and Yang, 2013). Therefore, the degree of dispersion determines the dispersion level. In 2007, Huang (2007) quantified the van der Waals forces (Lee et al., 2015) between nanoparticles for the first time by using the formula $F_A = \frac{AD}{24H^2}$, where A is the Hamaker constant (Diba et al., 2016) of the nanoparticle

in vacuum, H is the particle spacing, and D is the particle diameter. Coleman (2009) found that CNTs attract each other because of the van der Waals force interaction between adjacent carbon atoms, in which the potential energy of these paired interactions meets $V_r = -\frac{C}{r^6}$ (where r is the atomic spacing and C is a constant: $A = \pi^2\rho^2 C$, where ρ is the number of atoms in the unit volume in the cylinder) and A is the Hamaker constant, which depends on the total interaction force between adjacent CNTs and also the sum of the paired interaction forces of all carbon atoms. Coleman (2012) found that the theory of graphene exfoliation was similar to that of CNT exfoliation. These potential energies are larger than the paired interacting atoms and generally interact with molecules. The dispersant–solvent/graphene system involved in the liquid-phase dispersion of olefins also has an above potential energy, and the theoretical basis for achieving the successful exfoliation of graphene is to offset the above attraction. Coleman (2012) believed that the essence of graphene exfoliation is that the Hamaker constant was calculated to accurately quantify the van der Waals forces between graphene sheets. Although the researchers first used the developed parametric model and force–distance relationship to calculate the Hamaker constant using atomic force microscopy (AFM) analysis (Chu et al., 2017; Chiou et al., 2018), Gou et al. (2016) believed that the theoretical Hamaker constant of colloid should be determined by dynamic light scattering. In addition, for the ionic graphene dispersion system, when calculating the Hamaker constant by dynamic light scattering technique, the Hofmeister effect must be considered to obtain the accurate Hamaker constant, because different types of salt ions determine different Hofmeister effects (Zhou et al., 2017; Luo et al., 2018). It has certain advantages, but a standard method for determining the Hamaker constant is currently lacking. Therefore, the Hamaker constant theory needs to be further studied in the future.

Graphene Liquid-Phase Exfoliation Method

The main liquid-phase exfoliation methods include ultrasonic degradation (Narayan et al., 2017; Cai X. Z. et al., 2018), mechanical exfoliation (Su et al., 2011; Jung et al., 2015; Ping et al., 2017), and electrochemical exfoliation (Parvez et al., 2014; Jung et al., 2015; Shinde et al., 2016). In the study of the liquid-phase exfoliation of graphene, the most widely used method is to use natural flake graphite as raw material. In the dispersant–solvent system, graphite is first intercalated to obtain expanded graphite, and then different methods are employed to overcome the van der Waals force between graphite layers according to the Hamaker constant theory to achieve the exfoliation and dispersion of graphene (Dappe et al., 2006; Boström and Sernelius, 2012; Davidson et al., 2014; Lee et al., 2015). The dispersion mechanism and process are shown in **Figure 1**.

Ultrasonic Degradation

Ultrasonic degradation has the advantages of low cost and simple operation (Li et al., 2017), but long-term usage of ultrasonic graphene causes defects, and layer number renders the lamella radial size difficult to control (Khan et al., 2010) and enlarges the scale and the ultrasonic generator (Tian et al., 2017). The traditional ultrasonic degradation process is no longer adopted in present experimental studies and industrial production, and many studies aimed for improvement and innovation (Moorthy et al., 2015; Abo-Zahhad et al., 2016; Li et al., 2017; Narayan et al., 2017; Cai X. Z. et al., 2018; Gai et al., 2018). Gao et al. (2017) combined an ultrasonic generator with a supercritical reactor (**Figure 2**) by using ultrasonic degradation and supercritical CO_2 ($scCO_2$) excellent penetration of air to natural graphite in the $scCO_2$, H_2O, and ethanol system. High-quality graphene (>50%) was obtained in the mixed system. The method for industrial production provides a green, fast, and scalable way of graphene dispersion. Phiri et al. (2017) improved the traditional process of graphene preparation by ultrasonically exfoliating graphite in water medium. In the process of ultrasonic exfoliation, graphene was exfoliated and dispersed by means of a high shear colloidal mixer for 2 h to obtain a graphene dispersion with a concentration of up to 1.1 mg/ml. The graphene fractions prepared by ultrasonic peeling graphite for 100 h were separated by traditional process. Graphene dispersions of the same quality can be prepared in 0.5 h with the improved process. The graphene prepared by the improved process is analyzed by AFM and Raman. The dispersions contain plenty of defect-free and unmodified graphene layers. Hadi et al. (2018) mixed magnetic nanoparticles (Fe_3O_4) and graphite evenly during the preparation of graphene dispersion through the liquid-phase peeling of graphite. During ultrasonic exfoliation, the intense shear force between graphite nanosheets promotes the exfoliation of graphene, greatly shortens the ultrasonic time, and avoids long-term ultrasound bringing defects to graphene surface.

Mechanical Exfoliation

Because of the different parameters of the ultrasonic exfoliation process (e.g., time, frequency, power, and shape of the inner cavity), the experimental results are greatly affected (Río et al., 2017). At present, in the mechanical peeling process (including shearing and ball milling) (Deng et al., 2016; Liu Y. J. et al., 2018), the combination of shear and ball milling exfoliation process has been identified as the trend of replacing the ultrasonic peeling process in the future (Tour, 2014; Bonaccorso et al., 2016). Novoselov et al. (2004) first prepared graphene by the scotch tape stripping method and won the 2010 Nobel Prize in Physics. But the efficiency of this method is extremely limited to laboratory research (Yi and Shen, 2015). The advantage of mechanical exfoliation is that high-quality graphene can be obtained, but the mechanical exfoliation theory is more complicated than other stripping methods, and the stripping process is affected by many uncontrollable factors (e.g., the thickness of the graphene, and horizontal size).

Chen et al. (2012) used the mechanical peeling method in the experimental study. In the *N*-methyl pyrrolidone (NMP) system, the shear force produced by high-speed mechanical exfoliation interacts with van der Waals force between graphite sheets in an inclined 45° test tube (**Figure 3a**), resulting in relative slippage between graphite sheets, good peeling effect of the dispersion system assisted by NMP and overall dispersion. The process does not introduce defects in graphene (**Figures 3b–d**). Paton et al.

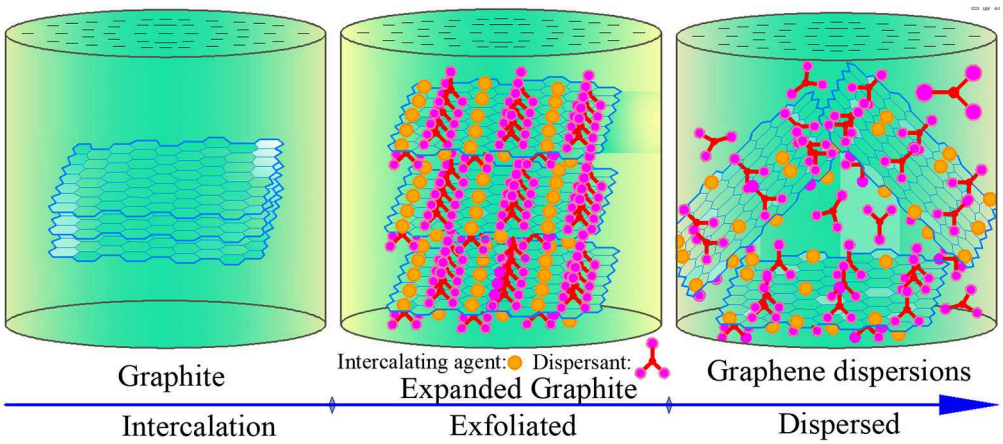

FIGURE 1 | Microstructure diagram of graphene exfoliation and dispersion by stripping graphite in liquid phase.

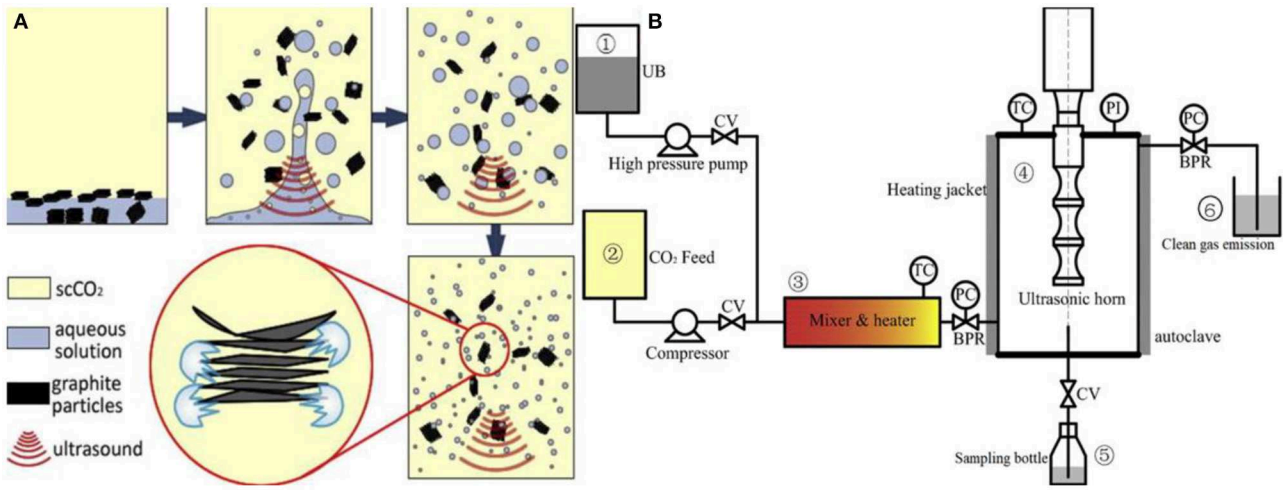

FIGURE 2 | (A) The $scCO_2$, aqueous solution, and graphite particle state are distributed before and after the ultrasonic wave is applied to the system. **(B)** Pilot plant for the large-scale production of graphene in $scCO_2$/polyvinylpyrrolidone (PVP)/H_2O systems by ultrasonic-assisted stripping of natural graphite (where UB is the ultrasonic bath, TC is the temperature controller, PI is the pressure indicator, and PC is pressure controller; BPR is the back-pressure regulator and CV is the check valve; ① is the raw material supply system, ② is the CO_2 feeding system, ③ is the heating/mixing system, ④ is the ultrasonic coupling supercritical reactor, ⑤ is the product collector, and ⑥ is the exhaust gas collector).

(2014) extended the theory of Chen et al. (2012) and proposed the theory of shear rate:

$$\gamma_{\min} = \frac{\left[\sqrt{E_{S,G}} - \sqrt{E_{S,L}}\right]^2}{\eta_L} \quad (1)$$

where $\gamma_{\min}$ is the shear rate, $E_{S,G}$ and $E_{S,L}$ are the surface energies of graphene and solvent, the surface energy of NMP is 69 $\frac{mJ}{m^2}$, η is the viscosity of the liquid, and L is the length of the graphite sheet. L = 300–800 nm of graphene was measured by transmission electron microscopy (TEM), and the minimum shear rate $\gamma_{\min} \approx 10^4\ s^{-1}$ was calculated. $E_{S,G}$ was calculated by Formula (1): $E_{S,G} = 70.5–71\ \frac{mJ}{m^2}$, which is very close to the surface potential energy ($E_{S,G} = 69\frac{mJ}{m^2}$) for the automatic exfoliation of graphene liquid phase. To verify the surface energy theory of graphene liquid-phase auto-exfoliation, many researchers have obtained the best surface energy through experiments, but the numerical values are different, and a unified theory is currently lacking (Kozbial et al., 2014). Single surface energy theory cannot completely explain the mechanism of graphene liquid-phase auto-exfoliation (Coleman, 2012) and thus has been replaced by the Hamaker constant theory.

Electrochemical Exfoliation

Electrochemical exfoliation method has become one of the most researched potentials of graphene liquid-phase exfoliation theory (Parvez et al., 2014) because of its advantages of being fast and has high efficiency, environmental protection, and low cost, etc. (Parvez et al., 2014; Artur and Paolo, 2016; Li et al., 2016; Ping et al., 2017). Su et al. (2011) exfoliated graphite by electrochemical stripping to prepare graphene dispersion,

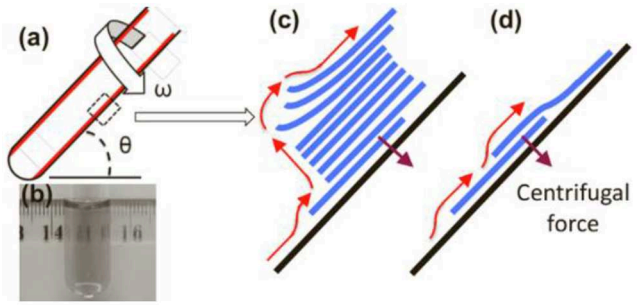

FIGURE 3 | (a) Schematic diagram of the vortex device (10 mm in diameter, 16 cm long, 45° inclined, graphite running at 7,000 rpm). **(b)** Photograph of a colloidal suspension of graphene obtained in NMP. **(c)** Schematic diagram of the stripping process. **(d)** Sliding on the inner surface of the rotating tube; the red arrow indicates the direction of the shear flow.

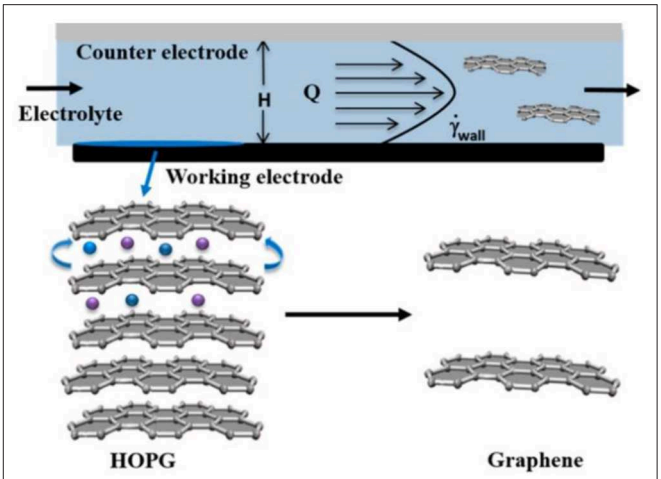

FIGURE 4 | Schematic of the experimental principle of an electrochemical microreactor. Graphite crystals were both reactor walls and working electrodes that apply an electric field at the same time as high shear. *H*, *Q*, and γ are the height between the two electrodes, the electrolyte flow rate, and the shear rate, respectively.

characterized by AFM, TEM, scanning tunneling microscopy (STM), Raman and attenuated total reflection–Fourier-transform infrared spectroscopy (ATR-FTIR). More than 60% of graphene in the dispersion was AB stack. Bilayer graphene has a lateral dimension of 30 μm on the surface, and its electrical properties were superior to those of reduced graphene oxide (rGO). Shinde et al. (2016) used hydrodynamics to prepare graphene by the shear-assisted electrochemical exfoliation method for the first time in the study of the electrochemical exfoliation of graphene. The graphene prepared at a high potential was thick and contained cracks. At low voltage (<1 V) potential, shear force had a more obvious assistant effect on electrochemical exfoliation (the exfoliation mechanism is shown in **Figure 4**). The monolayer, bilayer, and trilayer in the dispersion graphene occupied a high proportion. The Raman characterization showed only a few defects on the surface of graphene (I_D/I_G = 0.21–0.32), and these defects were distributed at the edge of graphene. Shi et al. (2018) demonstrated a non-electrified electrochemical exfoliation method to produce high-quality graphene (NEEG) sheets. By direct electrochemical reaction between graphite powders and metallic Li in 1 M of $LiPF_6$/propylene carbonate electrolyte, continuous graphite exfoliation is achieved with a high yield of excess 80% without any consumption of electric energy. The as-prepared NEEG has high quality with few defects (I_D/I_G = 0.45), a high C/O ratio of 27.74, and excellent electronic conductivity of 102.5 S/cm. As conductive additives in $Li_4Ti_5O_{12}$ electrode for lithium ion batteries, NEEG contributes to higher capacity and initial coulombic efficiency than common thermally rGO. Therefore, electrochemical exfoliation method is promising for large-scale production of high-quality graphene nanosheets (Liu Y. J. et al., 2018).

LIQUID-PHASE STABLE DISPERSION OF GRAPHENE

Liquid-Phase Stable Dispersion Mechanism of Graphene

The ultimate aim of the study on the stable dispersion of graphene in the liquid phase is to find the most suitable dispersant–solvent system to interact with graphene in many dispersant–solvent systems in order to improve the interfacial properties of graphene in liquid medium and realize the uniform and stable dispersion of graphene. Vallés et al. (2008) experimentally showed that the surface tension of the dispersant–solvent system suitable for the liquid-phase dispersion of graphene should be equal to the surface tension of graphene. Coleman (2009) first proposed the dispersion theory of surface energy in CNT dispersion, extended this theory to the theory of liquid-phase dispersion of graphene, and successfully measured the surface tension of graphene to be 70 mJ/m^2. Then, Catheline et al. (2011) used KC_8 intercalated graphite to prepare uniform graphene dispersion by liquid-phase exfoliation in NMP. Although the process of KC_8 dissolution could not explained, the Hansen dissolution coefficient theory was used in the NMP dispersion system. The reason for the uniform and stable dispersion of graphene was researched; that is, the free energy of the graphene layer intercalated by KC_8 was much less than the free energy between the original graphene sheets. Coleman (2012) continued to study the surface energy theory. In a series of solvents, graphite powder was ultrasonically exfoliated and dispersed at low power. The surface energy theory was not a strong basis for selecting the best dispersant–solvent system. In considering that not all dispersant–solvent systems have a surface energy close to 70 mJ/m^2, the graphene in the liquid-phase medium was automatically dispersed. Coleman proposed the HSP theory and expressed the content of HSP whose sum of squares is equal to the sum of the squares of the Hildebrand dissolution parameter δ, which satisfies

$$\delta_T^2 = \delta_D^2 + \delta_P^2 + \delta_H^2 \quad (2)$$

where δ_D, δ_P, and δ_H are the dispersibility, polarity, and hydrogen bond solubility parameters, respectively. Formula (2) shows that

the value of HSP must be accurately calculated and a suitable dispersant–solvent system must be selected to obtain stable dispersed graphene dispersions. This process allows graphene to be dispersed stably in liquid medium in the form of single or few layers. Based on the study of Coleman, Yi et al. (2013) extended the study of HSP. In liquid medium, the distance between solvent molecule 1 and solute molecule 2 was defined as $Ra = \sqrt{\left(4\left(\delta_{D1} - \delta_{D2}\right)^2 + \left(\delta_{P1} - \delta_{P2}\right)^2 + \left(\delta_{H1} + \delta_{H2}\right)^2\right)}$ [the parameters in this formula were the same as those in Formula (2)]. When Ra was closer, the solubility of HSP was the highest. The theory was used to analyze the acetone/water mixture system. When the mass fraction of acetone was 75%, the best HSP was obtained. Song et al. (2013) found that the non-covalent interaction between graphene and 1-pyridinebutyric acid (PBA) has the lowest degree of damage to the structure of graphene. The results of experiments on various dispersant–solvent systems showed that graphene exhibits the best dispersion in the PBA–acetone system. Song et al. (2013) considered that the interaction of δ_H and δ_H in HSP was the result of the calculation of $\delta_P + \delta_H = 17.0$, which satisfies the predicted value of HSP (generally $\delta_P + \delta_H = 13$–29). At the same time, inspired by the experimental conclusion of Park et al. (2009), graphene bound by non-covalent bonds can also be well-dispersed in the mixture of methanol and water ($\delta_P + \delta_H > 29$). Song et al. (2013) considered that COOH groups on PBA and liquid-phase systems can also be well-dispersed in the mixture of methanol and water ($\delta_P + \delta_H > 29$). Interaction occurs; and graphene, which was non-covalent bonded by PBA, was well-dispersed in liquid medium. At present, the HSP theory is the most breakthrough theory of liquid-phase stable dispersion of graphene. Its advantage is to accurately calculate the dispersibility and solubility of graphene in solvent–dispersant system. However, the theoretical calculation is complicated and requires high experimental analysis. It has not been widely used in practical experimental research and industrial production.

The concentration of graphene is a key parameter in the liquid-phase dispersion theory of graphene. However, many researchers failed to discuss the initial concentration of graphene, the volume of solvent, and the key parameters (e.g., time, rotating speed, power, and temperature) of liquid-phase exfoliation in the dispersion liquid system and to compare them with the graphene concentrations reported by other groups in the experimental discussion. For example, Yang and Yang (2018) used an electrochemical exfoliation method in the NMP system to strip a graphite rod intercalated with sodium sulfate to prepare a graphene dispersion and only reported the concentration of graphene in the dispersion (11.47 mg/ml). Obviously, it is meaningless to ignore the key parameters of the experiment to discuss graphene concentration. Fortunately, Artur and Paolo (2016) studied the graphene concentration in the graphene liquid-phase dispersion problem and discussed three important ratios: (1) mass ratio of starting graphite to graphene (Y, %); (2) ratio of single-layer graphene to multilayer graphene (W, %); and (3) ratio of single-layer graphene to the graphene dispersion system (V, %).

Liquid-Phase Stable Dispersion Method

π-π Interaction

In a review of the functionalization of non-covalent bonds of graphene, Georgakilas et al. (2016) reported the existence of π-π interactions: (1) π bonds exist between two molecules; (2) the interaction with two the geometry of the molecule is related; and (3) two molecules containing the π structure overlap, and the flatness of the surface of the nano-thin film of the two conjugated structures influences the π-π interaction. Wang et al. (2014) used the density functional theory of verified dispersion correction in combination with the zero-order symmetric adaptive perturbation theory to study the π-π interaction between graphene and aromatic molecules and to verify the dispersion-modified density functional theory. The zero-order symmetric adaptive perturbation theory of spin component scaling analyses the π-π interaction between graphene and aromatic molecules, which is believed to depend largely on the dispersion force and electrostatic interaction and is found to be more abundant. When a negative electron fluorine atom is substituted to an aromatic group, the π-π interaction becomes stronger and the liquid-phase dispersion property of graphene improves. Unfortunately, Wang et al. (2014) have only made a simple speculation on the π-π interaction and have not been able to further study it. In the field of liquid-phase dispersion of graphene, the nature of the interaction between π-π remains controversial to date (Ding et al., 2018). Wang X. D. et al. (2018) used strong non-covalent bonding (e.g., π-π interaction, hydrogen bonding, and GH–C interaction) between molecules to prevent the agglomeration of rGO lamellae and obtained uniformly dispersed rGO/poly(vinyl alcohol) (PVA) nanocomposites, as shown in **Figure 5**. The mechanical properties (including Young's modulus and tensile strength) and thermal properties of the composites can be significantly improved by adding a small amount of rGO into PVA.

Only some researchers speculated a reason for the formation of electron-rich exchange between the π-conjugated structure of graphene surface and aromatic molecules. In addition, the π-π interaction between aromatic molecules and graphene not only improves the liquid-phase dispersion but also adjusts the band gap to precisely control its electronic properties (Nduwimana and Wang, 2009; Zhang et al., 2011; Deka and Chowdhury, 2016). The π-π interaction method includes pyrene derivatives, biomolecules, CNT, and GO.

Pyrene Derivatives

Pyrene derivatives were first used in the liquid-phase dispersion of CNTs. Most researchers used NMP as solvent and pyrene derivatives as dispersant to prepare CNTs (Ehli et al., 2006; Meuer et al., 2009) by ultrasound degradation. However, the liquid-phase dispersion theory for dispersing CNT on curved surfaces is not necessarily applicable to the liquid-phase dispersion of graphene on planar surfaces (Abo-Zahhad et al., 2016). O'Neill et al. (2011) used aminoethyl pyrene ($PyMeNH_2$) and 1,3,6,8-pyrene tetrasulfonate [$Py(SO_3)_4$] as dispersants to stabilize the dispersion of monolayer graphene in aqueous solution and prepared transparent conductive films. Parviz et al. (2012) used various pyrene derivatives to disperse graphene

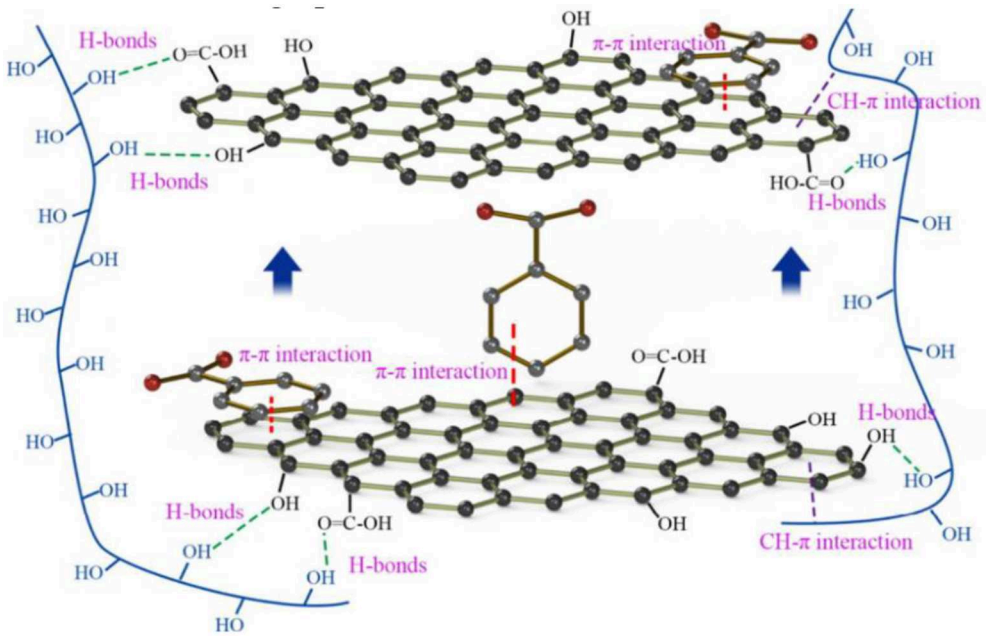

FIGURE 5 | Schematic diagram of the interaction among the reduced graphene oxide (rGO) sheets, poly(vinyl alcohol) molecules, and poly(sodium 4-styrenesulfonate) molecules (Wang X. D. et al., 2018).

in a water system. The graphene dispersed in the pyrene derivative system had a dispersion stability of several months. Among different pyrene derivative systems, the effect of the sodium pyrene sulfonate (Py-SASS) dispersion system was the best. As shown in **Figure 6A**, the concentration of graphene in liquid medium was as high as 0.8–1 mg/ml, as shown in **Table 1**. Parviz et al. (2012) found that dispersants were automatically adsorbed onto the surface of graphene when the polarity of solvents and dispersants was significantly different. A study on the role of pyrene derivative functional groups in liquid-phase dispersion found that functional groups with high electronegativity effectively promote the adsorption of dispersants onto the surface of graphene (**Figure 6B**). Zhang (2016) synthesized a new dispersant, sodium pyrene-butane-1-sulfonate (Py-C_4-SASS), for the stripping and dispersion of graphene in aqueous media. Parviz et al. (2012) found through a comparative analysis that the new dispersant and Py-SASS, a bismuth-based graphene dispersant, could stably diffuse graphene in an aqueous medium. The exfoliation effect of the two dispersant systems was characterized by Raman and AFM spectroscopic methods (**Figure 7A**). The ratio of single layer and less layer ($\leq$4 layers) was extremely high, and the radial dimension (0.5 μm) of Py-C_4-SASS-assisted exfoliated graphene is larger than the radial dimension (0.2 μm) of Py-SASS-assisted exfoliation. The UV-Vis spectroscopy was also performed to test the two dispersion systems. The concentration of graphene in the Py-C_4-SASS system was twice that of the Py-SASS system (**Figure 7B**). Unfortunately, Zhang failed to demonstrate the underlying cause of the difference in the ability to strip and disperse graphene between Py-SASS and Py-C_4-SASS. Chen C. et al. (2017) used poly(2-butylaniline) (P2BA) as a dispersant to peel off a few layers of graphene in organic solvents. The strong π-π interaction between P2BA with π conjugate structure and graphene solves the problem of graphene agglomeration in organic solvents.

Biomolecules

Among the various reagents that interact with graphene, the advantages of biomolecules are low cost, environmental friendliness, and biocompatibility (Liu et al., 2017). Biomolecules that can interact with graphene include proteins and nucleotides (Ehli et al., 2006; Zhang et al., 2011; Deka and Chowdhury, 2016) (DNA/RNA), polysaccharides, and bile salts (Chang et al., 2010; Paredes and Villar-Rodil, 2016). The non-covalent bonding of protein and graphene in an aqueous medium produces a strong steric hindrance effect, which sharply reduces the free energy of graphene in the liquid medium, preventing the mutual graphene layers from each other. The rate of proximity is important to achieve uniform and stable dispersion of the graphene liquid phase (Bourlinos et al., 2009; Laaksonen et al., 2010). Flavin mononucleotides can also be strongly adsorbed onto the surface of rGO (Ayán-Varela et al., 2015; Yoon et al., 2015; Munuera et al., 2016). For example, Vashist and Luong (2015) studied target proteins and found that nucleotides DNA/RNA were highly adsorbed onto the surface of electrochemically and thermochemically reduced rGO. Compared with the surfactant dispersion system, although the concentration of graphene was much lower in the biomolecular system than in the surface active system (Seo et al., 2011; Notley, 2012; Zhu et al., 2014), the advantages of the nucleotide (DNA/RNA) dispersion system,

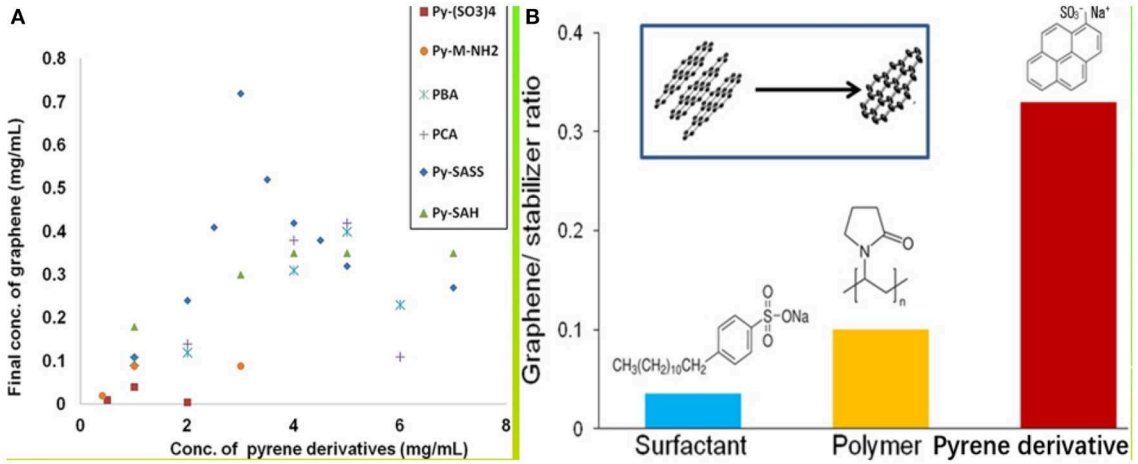

FIGURE 6 | (A) Dispersion of graphene by each pyrene derivative. **(B)** Dispersion of graphene by different negatively charged dispersants.

TABLE 1 | Summary of dispersant, polymer and pyrene derivatives on graphene dispersibility.

Dispersants	Dispersant concentration (mg/ml)	Initial expanded graphite concentration (mg/ml)	Final graphene concentration (mg/ml)	Graphene to dispersant concentration ratio	Dispersant molecular structure
SDBS	6	50	0.22 ± 0.03	0.036	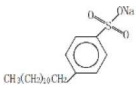
PVP	10	50	1 ± 0.1	0.1	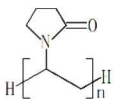
Py-SASS	3	50	1 ± 0.05	0.33	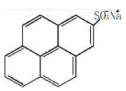

SDBS, sodium dodecylbenzenesulfonate; PVP, polyvinylpyrrolidone; Py-SASS, sodium pyrene sulfonate.

such as biocompatibility and low cost, are not comparable with those of other dispersion systems (Georgakilas et al., 2012; Ayan-Varela et al., 2017).

Carbon Nanotubes

As a 1D nanomaterial, CNTs form a six-membered ring structure from carbon atoms and contain plenty of conjugated large π bonds (Ehli et al., 2006; Li et al., 2018). It can interact with graphene through π-π interaction to form a steric hindrance effect (Zhang and Huang, 2000; Zhou and Zhang, 2015; Cao et al., 2017) to achieve the stable liquid-phase dispersion of graphene. Yue et al. (2014) prepared epoxy resin fillers by ultrasonic degradation. A study on the dispersion effects of graphene nanoplates (GNPs), CNTs, and GNP/CNT in liquid medium by the volume sedimentation method found that the GNP/CNT (2:8 mixture) system exhibits the best effect of graphene stable dispersion. As shown in **Figure 8a**, scanning electron microscopy (SEM) characterization showed that GNP and CNTs can prevent each other from agglomerating. Pure GNP system has higher dispersion than the GNP/CNT system, as shown in **Figures 8b–g**. Ji et al. (2016) made use of sulfonated CNT (SCNT) and successfully prepared a high concentration of graphene. SCNT played a tremendous role in not only suppressing the agglomeration of graphene but also bridging graphene sheets to improve the interlamellar conductivity. Compared with other dispersant systems in the liquid-phase dispersion of graphene, CNTs and graphene are excellent carbon nanomaterials, and their mixed dispersion system has a wide range of applications in energy storage and conduction (Cui and Li, 2002; Dimitrios et al., 2006; Tang et al., 2014; Zhao et al., 2014; Ji et al., 2016). In the process of preparing PS/PMMA composites, Chen J. W. et al. (2017) developed an effective thermodynamic method to balance the π-π interaction between PS and multi-walled CNTs and the PMMA between multi-walled

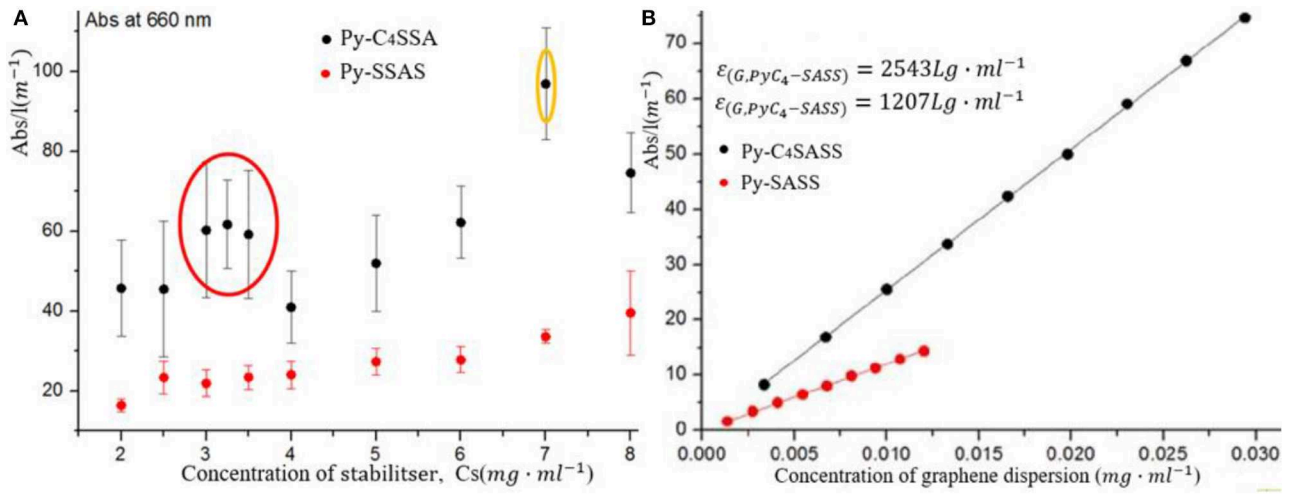

FIGURE 7 | Dispersion of graphene by pyrene derivatives sodium pyrene sulfonate (Py-SASS) and sodium pyrene-butane-1-sulfonate (Py-C_4-SASS). **(A)** Comparison of the stripping ability of the two dispersants to graphene. **(B)** UV-Vis test analysis results of the two dispersant systems.

CNTs. The dipole–dipole interaction with the carboxyl group enables uniform dispersion of the multi-walled CNTs in the composite. Fortunately, the mechanism of the π-π interaction can also be analyzed.

Graphene Oxide

GO is amphiphilic (Geng et al., 2017) and reduces the solid–liquid interfacial energy in liquid media (Tian et al., 2011; Shao et al., 2014). Tung et al. (2016) used GO as a dispersant to prepare graphene by stripping graphite in liquid phase. GO as a surfactant not only assists graphite stripping but also renders it uniformly and stably dispersed in liquid phase through the π-π interaction. UV-Vis, SEM, and TEM analyses showed that the stripping yield of single-layer and less-layer graphene in the dispersion is high (40% of the initial graphite mass), and the quality of graphene is excellent (C/O = 21.5, $\frac{I_D}{I_G} = 0.12$, conductivity $6.2 \times 10^4 \frac{m}{s}$).

Interaction With Polymers

The non-covalent bond with polymers can achieve both the dispersion of the graphene inorganic solvent and the dispersion of the organic solvent. For example, Choi et al. (2010) first prepared rGO dispersions in pure water by the chemical reduction of GO. Amino groups on polystyrene capped by polymer amine were successfully grafted with carboxylic acid groups remaining on the surface of rGO, forming non-covalent bonds with graphene and transforming graphene from the aqueous phase to the organic phase by ultrasonic degradation. After FTIR and Raman were analyzed, the protonated amino group of polystyrene interacts with the carboxylic acid group on the surface of rGO, realizing non-covalent bonding with graphene and improving the dispersion of graphene in organic media. Tchernook et al. (2014) used polyethylene nanoparticles to add a surfactant to the aqueous system to polymerize, and its dispersion process is shown in **Figure 9**. The test proves that the graphene is not modified in the aqueous polyethylene/graphene mixed system and the polyethylene nanoparticles disperse the graphene. It has a steric hindrance effect (Li et al., 2012) to achieve the uniform and stable dispersion of graphene. Chen J. et al. (2017) prepared water-borne graphene dispersions from graphite by electrochemical exfoliation with alkaline solution of hydrolyzed styrene–maleic anhydride copolymer as electrolyte. X-ray powder diffraction (XRD), AFM, and TEM analyses showed that monolayer graphene exists in graphene in the dispersions. FTIR and thermogravimetric analysis demonstrated that the hydrolyzed styrene–maleic anhydride polymer is combined with the graphene surface by a non-covalent bond to obtain a high concentration (>1 mg/ml) and stable aqueous graphene dispersion.

Surfactant Interaction

Surfactants can adjust the surface energy of graphene and different media to promote its stable dispersion. Surfactants have been widely studied as effective agents for the liquid-phase stable dispersion of graphene (Coleman, 2012; Zhao H. L. et al., 2018). Wei et al. (2011) compared the dispersing ability of different surfactants to graphene in the experiment of preparing graphene dispersion solution by exfoliation graphite in liquid phase. Results show that non-ionic surfactant PVP exerts greater dispersing ability, better biocompatibility, environmental friendliness, and lower cost than do other dispersants. Vadukumpully et al. (2011) applied the cationic surfactant hexadecyl trimethyl ammonium bromide (CTAB) as a dispersing agent to ultrasonically exfoliate graphite in a glacial acetic acid system, and they found that a large number of single-layer and less-layer graphene are stably dispersed in the *N*, *N*-dimethylformamide–CTAB system. Tkalya et al. (2012) reviewed the liquid-phase dispersion theory of graphene by surfactants and summarized the surface active agents, including CTAB, PVP, sodium dodecyl sulfate, sodium dodecylbenzenesulfonate (SDBS), lithium dodecyl sulfate, tetradecyl trimethyl ammonium

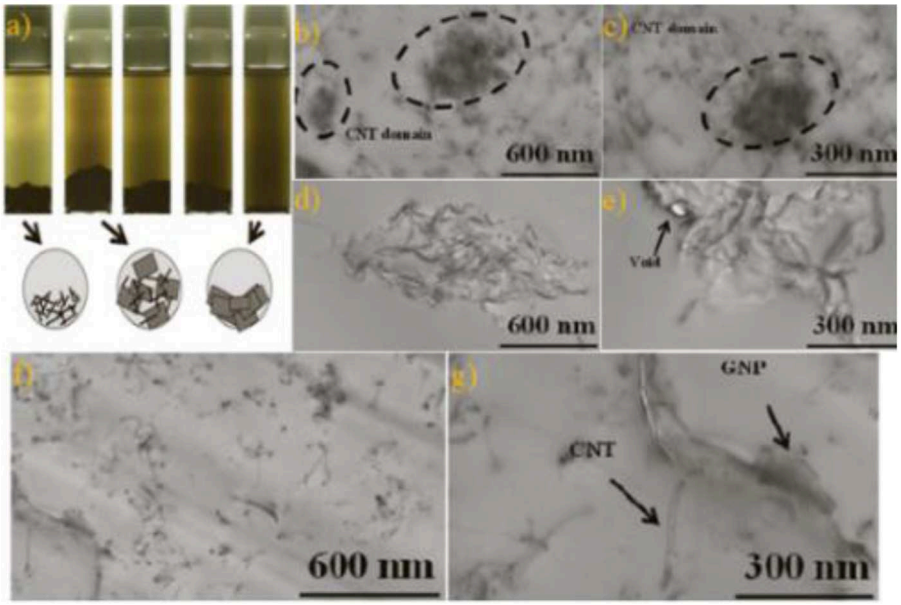

FIGURE 8 | (a) After 72 h of ultrasonic exfoliation, carbon filler/tetrahydrofuran suspension were CNT, CNT:GNP = 8:2, CNT:GNP = 4:6, CNT:GNP = 2:8, and GNP with 0.1 mg/ml of filler concentration as shown in the images, with the diagrams of sediment fillers in various filler suspensions. **(b,c)** CNT/epoxy composite SEM diagrams. **(d,e)** GNP/epoxy composite SEM diagrams. **(f,g)** CNT:GNP = 8:2/epoxy composite SEM diagrams. CNT, carbon nanotube; GNP, graphene nanoplate; SEM, scanning electron microscopy.

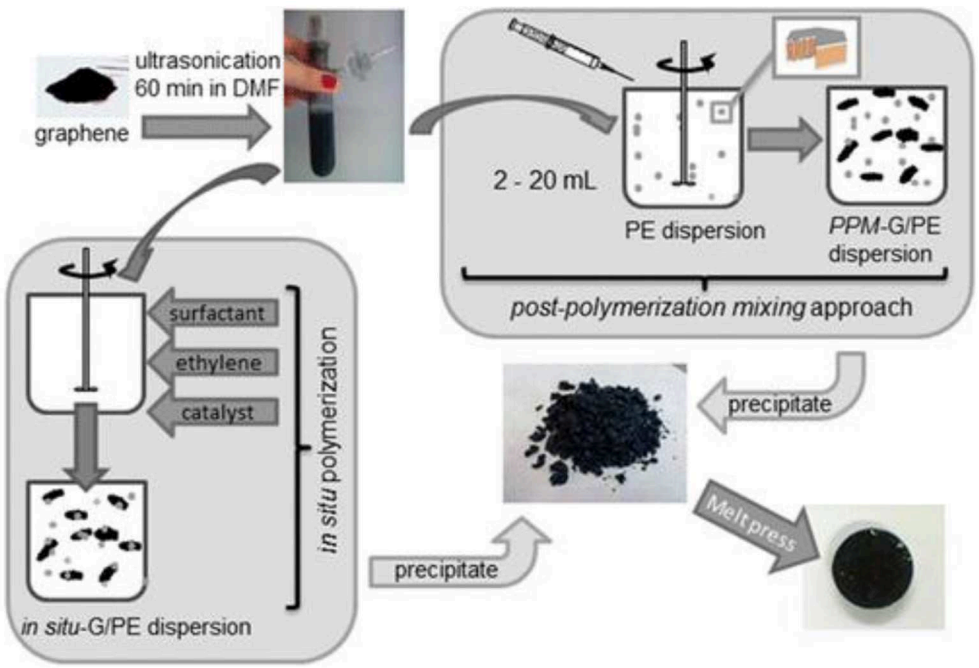

FIGURE 9 | Approaches to aqueous polyethylene/graphene composite dispersions by *in situ* polymerization, postpolymerization mixing, and precipitation to yield solid composite material (Tchernook et al., 2014).

bromide, sodium cholate, sodium deoxycholate, taurocholic acid, Tween 20, Tween 80, and Triton X-100, among others. Wang et al. (2017) used spray coating to prepare graphene films on glass and n-Si substrates through ultrasonic degradation and utilized anionic surfactant SDBS as a dispersant to prepare graphene dispersion in pure water. The liquid was subjected

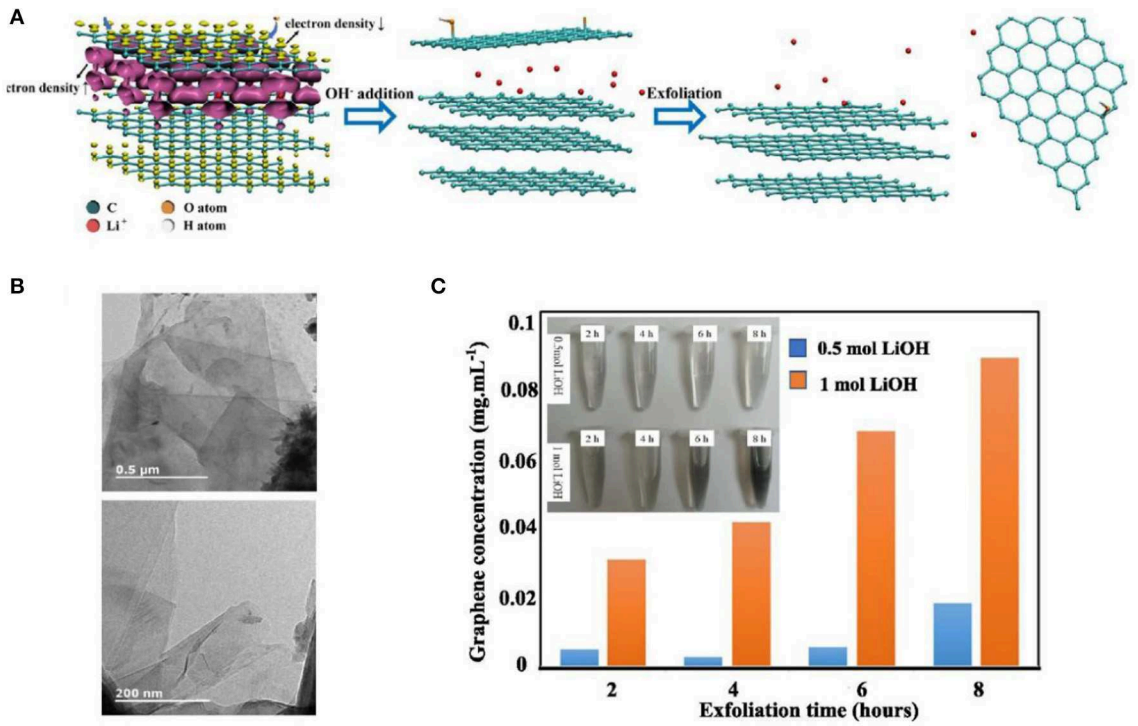

FIGURE 10 | (A) Synthetic strategy diagram of the Li^+-OH^- stripping system. The purple and yellow surfaces in the left image represent the +0.002 and −0.002 e/Bohr^3 isosurfaces of the electron density difference caused by Li^+ embedding. **(B)** Transmission electron microscopy (TEM) image of the exfoliated graphene sheet. **(C)** Relationship between the concentration of graphene and the synergistic effect of LiOH and the peeling time. The inset is a prepared aqueous graphene suspension.

to UV-Vis analysis to obtain a stable graphene dispersion with a concentration of 15% SDBS. The surface morphology of the graphene has a blade-like edge structure. At the same time, the transmittance of visible light is more than 82% (about seven layers) (Selvakumar et al., 2018). This result proves that SDBS has strong exfoliation and stable dispersing ability to graphene.

The surfactant system exerts the best dispersion effect on graphene liquid-phase dispersion, but it cannot avoid introducing other side effects to the dispersion liquid system because of its own defects while solving graphene liquid-phase stable dispersion (De et al., 2010; Bepete et al., 2017; Shabafrooz et al., 2018). For example, Tkalya et al. (2012) found that non-ionic surfactants have long hydrophilic end and large volume characteristics. While preventing graphene agglomeration, the large volume effect of non-ionic surfactants can also lead to large distance between adjacent graphene sheets, which affects the conductivity of graphene and the permeability of graphene membranes in the dispersion system. Bepete et al. (2017) applied mechanical exfoliation theory to peel graphite after intercalation of the compound in water to obtain graphenide (negatively charged graphene) solutions. By using the advantages of outstanding volatility of tetrahydrofuran, graphene, and tetrahydrofuran can be mixed in water at room temperature to obtain a high concentration (0.16 g/L) and uniformly dispersed aqueous graphene dispersion. Bellani et al. (2019) prepared graphene dispersion with high concentration and excellent dispersion stability in NMP by wet-jet grinding exfoliation and solvent-exchange process. Compared with traditional exfoliation and dispersion technologies (e.g., ultrasonic exfoliation and mechanical peeling), the above process extremely improved the exfoliated efficiency of graphene and satisfied the industrial requirement of large-scale preparation graphene. Although the dispersion of graphene is not prepared by using any surfactant, the large scale makes use of tetrahydrofuran, and NMP in the industry poses a certain safety hazard to human beings (Rodriguez-Laguna et al., 2018; Shabafrooz et al., 2018).

Therefore, the future theory of choosing green dispersants or avoiding using dispersants is the focus of the study on graphene liquid dispersion. For example, Zhang et al. (2018) exfoliated and dispersed graphene with nanocrystalline cellulose (NCC). The addition of NCC considerably reduces the deposition of graphene in the dispersion system. The NCC dispersion method is an efficient, green, and scalable method for preparing graphene fractions. The method of dispersing liquid has a wide potential for the industrial application of graphene in the future. Wang S. F. et al. (2018) used Li^+ and OH^- between graphene sheets. The positive charge of Li^+ moves to the adjacent C atoms, and the adjacent OH^- interacts with it, forming a hydroxyl group added to the surface of the graphene and increasing the hydrophilicity of the graphene (**Figure 10A**). The graphene dispersion in an aqueous medium was improved without using a dispersant, and

a graphene dispersion having a concentration of 0.09 mg/ml was prepared (**Figures 10B,C**).

Hydrogen Bond Interaction

Hydrogen bonding is a strong intermolecular force (bonding energy is 5–30 kJ/mol). The formation of intermolecular hydrogen bonds is profitable to the dispersion and dissolution between substances (Wang H. et al., 2018). Generally, the certain quantitative oxygen-containing groups will remain on the surface of graphene prepared by oxidation–reduction method (Aradhana et al., 2018) and ultrasonic graphite in water for a long time (Li et al., 2019). The oxygen-containing groups can produce strong hydrogen bond with dispersant–solvent system to improve the interfacial properties of graphene and achieve stable dispersion of graphene in liquid phase (Xu et al., 2017; Qin et al., 2018). For example, Yang X. M. et al. (2010) prepared a PVA/graphene mixture by dispersing rGO uniformly and stably in PVA. FTIR analysis was carried out because the residual oxygen-containing functional groups (such as carboxyl and hydroxyl) on the surface of rGO were combined with hydroxyl groups in PVA through hydrogen bonding, and the liquid-phase dispersion of graphene was well realized. León et al. (2013) used melamine as a dispersant to peel graphite in different liquid media (including organic solvents and aqueous solutions) by ball milling to obtain graphene dispersions with good dispersion stability. In the same solvent system, the exfoliation and dispersion ability of graphite with electron-rich benzene derivatives and triazine derivatives were tested, respectively. The present equivalent benzene derivatives do not exhibit the ability of peeling and dispersing graphite with melamine in the same solvent system. However, the aminotrigine system has a strong peeling and dispersing ability for graphene. The analysis and calculation showed that the aminotrigine derivatives could form a wide range of hydrogen bond 2D structures on the surface of graphene and has a good peeling and dispersing ability for graphene. The formation of hydrogen bonding makes it possible for the multi-point interaction of graphene surface in liquid medium. The stable combination of dispersant and oxygen-containing groups on graphene surface (as indicated by the green dotted line in **Figure 5**) can improve the dispersion stability of graphene in liquid medium.

SUMMARY AND OUTLOOK

In recent years, the most breakthrough theories in the study of liquid-phase stripping and stable dispersion of graphene are the Hamaker constant and the HSP. The two theories reveal the essence of graphene liquid-phase exfoliation and stable dispersion from the intermolecular force and the interfacial force between solute and solvent, respectively. It is also one of the important approaches to solve the problem of graphene agglomeration and realize the uniform and stable dispersion of graphene liquid phase. Coleman (2012) proposed the Hamaker constant theory to quantify the van der Waals force between graphene lamellae, and the HSP theory was used to analyze the relationship between different dispersant–solvent systems and the interface of graphene. However, the Hamaker constant theory still cannot accurately calculate the van der Waals force between graphene sheets. The theoretical calculation of the Hansen dissolution coefficient is complex, and the level of experimental analysis is high. Therefore, certain challenges remain in the theoretical study of liquid-phase exfoliation and dispersion of graphene. Among the many methods of stable dispersion of graphene, the π-π interaction provides a good protection for the original properties of graphene and an ideal stable dispersion effect. However, the essential mechanism of the π-π interaction is unclear. Only some researchers speculated that the π-conjugated structure on graphene surface is caused by the electron-rich exchange phenomenon produced by aromatic molecules. The real reason for the π-π interaction remains unclear. In summary, the current research on the liquid-phase stripping and stable dispersion theory of graphene is not comprehensive enough. Future studies should focus on solving the problem of graphene dispersion in nanomaterial research and practical industrial applications.

AUTHOR CONTRIBUTIONS

LLi, LJ, MZ, and YM jointly determined the research theme. LLi, SY, and LJ organized the database. LLi, MZ, XL, and LLiu conducted statistics and analysis. LLi, LJ, and MZ wrote the first draft. HZ, ZM, and ZL wrote part of the first draft. All authors participated in the revision of the manuscript, read, and approved the submitted version.

FUNDING

We are grateful for the financial support from the Guangxi Natural Fund (no. 2018GXNSFAAI38174) and Liuzhou Science and Technology Plan Project (no. 2018CB10508).

REFERENCES

Abo-Zahhad, E. M., El-Shazly, A. H., and El-Kady, M. F. (2016). Synthesis and characterization of nanomagnetic graphene via co-precipitation technique with aid of ultrasound. *Mater. Sci. Forum* 860, 21–24. doi: 10.4028/www.scientific.net/MSF.860.21

Alecrim, V., Zhang, R. Y., Hummelgård, M., Andres, B., Dahlström, C., Norgren, M., et al. (2015). *Exfoliated Layered Materials for Digital Fabrication*. Salt Lake City, UT: Society for Imaging Science and Technology.

Allen, M. J., Tung, V. C., and Kaner, R. B. (2010). Honeycomb carbon: a review of graphene. *Chem. Rev.* 110, 132–145. doi: 10.1021/cr900070d

Aradhana, R., Mohanty, S., and Nayak, S. K. (2018). Comparison of mechanical, electrical and thermal properties in graphene oxide and reduced graphene oxide filled epoxy nanocomposite adhesives. *Polymer* 141, 104–123. doi: 10.1016/j.polymer.2018.03.005

Artur, C., and Paolo, S. (2014). Graphene via sonication assisted liquid-phase exfoliation. *Chem. Soc. Rev.* 43, 381–398. doi: 10.1039/C3CS60217F

Artur, C., and Paolo, S. (2016). Supramolecular approaches to graphene: from self-assembly to molecule-assisted liquid-phase exfoliation. *Adv. Mater*. 28, 6030–6051. doi: 10.1002/adma.201505371

Ayán-Varela, M., Paredes, J. I., Guardia, L., Villar-Rodil, S., Munuera, J. M., Díaz-González, M., et al. (2015). Achieving extremely concentrated aqueous dispersions of graphene flakes and catalytically efficient graphene-metal nanoparticle hybrids with flavin mononucleotide as a high-performance stabilizer. *ACS Appl. Mater. Interf.* 7, 10293–10237. doi: 10.1021/acsami.5b00910

Ayan-Varela, M., Perez-Vidal, O., Paredes, J. I., Munuera, J. M., Villar-Rodil, S., Diaz-Gonzalez, M., et al. (2017). Aqueous exfoliation of transition metal dichalcogenides assisted by DNA/RNA nucleotides: catalytically active and biocompatible nanosheets stabilized by acid-base Interactions. *ACS Appl. Mater. Inter.* 9, 2835–2845. doi: 10.1021/acsami.6b13619

Bellani, S., Petroni, E., Del Rio Castillo, A. E., Curreli, N., Martín García, B., Oropesa Nuñez, R., et al. (2019). Scalable production of graphene Inks via wet-jet milling exfoliation for screen-printed micro-supercapacitors. *Adv. Funct. Mater*. 29, 1807659–1807673. doi: 10.1002/adfm.201807659

Bepete, G., Anglaret, E., Ortolani, L., Morandi, V., Huang, K., Pénicaud, A., et al. (2017). Surfactant-free single-layer graphene in water. *Nat. Chem*. 9, 347–352. doi: 10.1038/nchem.2669

Bonaccorso, F., Bartolotta, A., Coleman, J. N., and Backes, C. (2016). 2D-Crystal-based functional inks. *Adv. Mater*. 28, 6136–6166. doi: 10.1002/adma.201506410

Boström, M., and Sernelius, B. E. (2012). Repulsive van der Waals forces due to hydrogen exposure on bilayer graphene. *Phys. Rev. A* 85:012508. doi: 10.1103/PhysRevA.85.012508

Bourlinos, A. B., Georgakilas, V., Zboril, R., Steriotis, T. A., Stubos, A. K., and Trapalis, C. (2009). Aqueous-phase exfoliation of graphite in the presence of polyvinylpyrrolidone for the production of water-soluble graphenes. *Solid. State. Commun*. 149, 2172–2176. doi: 10.1016/j.ssc.2009.09.018

Brownson, D. A. C. (2013). Graphene electrochemistry: fundamentals through to electroanalytical applications. *Chem. Soc. Rev*. 41, 6944–6976. doi: 10.1039/c2cs35105f

Cai, X. Z., Jiang, Z. Y., Zhang, X. R., and Zhang, X. X. (2018). Effects of tip sonication parameters on liquid phase exfoliation of graphite into graphene nanoplatelets. *Nanoscale Res. Lett*. 13:241. doi: 10.1186/s11671-018-2648-5

Cai, Z. Y., Liu, B. L., Zou, X. L., and Cheng, H.-M. (2018). Chemical vapor deposition growth and applications of two-dimensional materials and their heterostructures. *Chem. Rev*. 118, 6091–6133. doi: 10.1021/acs.chemrev.7b00536

Cao, H., Jian, Y.-S., Ma, J. Y., and Jian, Y. L. (2014). Research of graphene used for li-ion batteries. *Chin. Battery Ind.* 19, 142–144. doi: 10.3969/j.issn.1008-7923.2014.03.008

Cao, R. C., Wei, X. F., Wang, Q., and Zhang, H. (2017). Research progress on dispersion technique of water-based ink. *Fine Chem.* 34, 242–249. doi: 10.13550/j.jxhg.2017.03.001

Cao, Y. C., and Guo, M. M. (2016). Graphene materials and its applications. *Petrochem. Technol.* 45, 1149–1159. doi: 10.3969/j.issn.1000-8144.2016.10.001

Catheline, A., Vallés, C., Drummond, C., Ortolani, L., Morandi, V., Marcaccio, M., et al. (2011). Graphene solutions. *Chem. Commun*. 47, 5470–5472. doi: 10.1039/c1cc11100k

Chang, H. X., Tang, L. H., Wang, Y., Jiang, J. H., and Li, J. H. (2010). Graphene fluorescence resonance energy transfer aptasensor for the thrombin detection. *Anal. Chem*. 82, 2341–2346. doi: 10.1021/ac9025384

Chen, C., Qiu, S. H., Cui, M. J., Qin, S. L., Yan, G. P., Zhao, H. C., et al. (2017). Achieving high performance corrosion and wear resistant epoxy coatings via incorporation of noncovalent functionalized graphene. *Carbon* 114, 356–366. doi: 10.1016/j.carbon.2016.12.044

Chen, J., Lu, H. Y., Chen, Y., Tao, Z. Z., and Shao, M. J. (2017). Stable aqueous dispersion of polymer functionalized graphene sheets from electrochemical exfoliation for anticorrosion application. *Colloid Polym. Sci.* 295, 1951–1959. doi: 10.1007/s00396-017-4173-y

Chen, J. W., Cui, X. H., Zhu, Y. T., Jiang, W., and Sui, K. Y. (2017). Design of superior conductive polymer composite with precisely controlling carbon nanotubes at the interface of a co-continuous polymer blend via a balance of π-π interactions and dipole-dipole interactions. *Carbon* 114, 441–448. doi: 10.1016/j.carbon.2016.12.048

Chen, X. J., Dobson, J. F., and Raston, C. L. (2012). Vortex fluidic exfoliation of graphite and boron nitride. *Chem. Commun*. 48, 3703–3705. doi: 10.1039/c2cc17611d

Cheng, C. G., Jia, P., Xiao, L. H., and Geng, J. X. (2019). Tandem chemical modification/mechanical exfoliation of graphite: scalable synthesis of high-quality, surface-functionalized graphene. *Carbon* 145, 668–676. doi: 10.1016/j.carbon.2019.01.079

Cheng, L. Q., Liu, Y. L., Zhang, J. X., Yuan, D. S., Xu, C. W., and Sun, G. H. (2006). Synthesis and application of spherical structured carbon materials. *Prog. Chem*. 18, 1298–1304. doi: 10.3321/j.issn:1005-281X.2006.10.006

Cheng, M. H. (1998). The development trend of new carbon materials. *Mater. Rep.* 12, 5–9.

Chiou, Y.-C., Olukan, T. A., Almahri, M. A., Apostoleris, H., Chiu, C. H., Lai, C.-Y., et al. (2018). Direct measurement of the magnitude of the van der Waals interaction of single and multilayer graphene. *Langmuir* 34, 12335–12343. doi: 10.1021/acs.langmuir.8b02802

Choi, E. Y., Han, T. H., Hong, J. H., Ji, E. K., and Sang, O. K. (2010). Noncovalent functionalization of graphene with end-functional polymers. *J. Mater. Chem.* 20, 1907–1912. doi: 10.1039/b919074k

Chu, L. Y., Korobko, A. V., Cao, A. P., Sachdeva, S., Liu, Z., de Smet, L. C. P. M., et al. (2017). Mimicking an atomically thin "vacuum spacer" to measure the Hamaker Constant between graphene oxide and silica. *Adv. Mater. Interfaces* 4:160495. doi: 10.1002/admi.201600495

Coleman, J. N. (2009). Liquid-phase exfoliation of nanotubes and graphene. *Adv. Funct. Mater*. 23, 3680–3695. doi: 10.1002/adfm.200901640

Coleman, J. N. (2012). Liquid exfoliation of defect-free graphene. *Accounts Chem. Res*. 46, 14–22. doi: 10.1021/ar300009f

Coletti, C., Forti, S., Principi, A., Emtsev, K. V., Zakharov, A. A., Daniels, K.M., et al. (2013). Revealing the electronic band structure of tri-layer graphene on SiC: an angle-resolved photoemission study. *Phys. Rev. B* 88:155439. doi: 10.1103/PhysRevB.88.155439

Cui, J. S., and Zhou, S. X. (2018). High-concentration self-cross-linkable graphene dispersion. *Chem. Mater*. 30, 4935–4942. doi: 10.1021/acs.chemmater.8b00884

Cui, S., and Li, H. Y. (2002). Research actualities of preparing carbon nanotubes. *Chem. Ind. Eng.* 19, 59–64.

Dappe, Y. J., Basanta, M. A., Flores, F., and Ortega, J. (2006). Weak chemical interaction and van der waals forces between graphene layers: a combined density functional and intermolecular perturbation theory approach. *Phys. Rev. B* 74:205434. doi: 10.1103/PhysRevB.74.205434

Davidson, E. R. M., Klimes, J., Alfè, D., and Michaelides, A. (2014). Cooperative interplay of van der waals forces and quantum nuclear effects on adsorption: H at graphene and at coronene. *ACS Nano* 8, 9904–9913. doi: 10.1021/nn505578x

De, S., King, P. J., Lotya, M., O'Neill, A., Doherty, E. M., Hernandez, Y., et al. (2010). Flexible, transparent, conducting films of randomly stacked graphene from surfactant-stabilized, oxide-free graphene dispersions. *Small* 6, 458–464. doi: 10.1002/smll.200901162

Deka, M. J., and Chowdhury, D. (2016). Tuning electrical properties of graphene with different π-stacking organic molecules. *J. Phys. Chem. C* 120, 4121–4129. doi: 10.1021/acs.jpcc.5b12403

Deng, S., Qi, X.-D., Zhu, Y.-L., Zhou, H.-J., Chen, F., and Fu, Q. (2016). A facile way to large-scale production of few-layered graphene via planetary ball mill. *Chinese J. Polym. Sci.* 34, 1270–1280. doi: 10.1007/s10118-016-1836-y

Diba, M., Fam, D. W. H., Boccaccini, A. R., and Shaffer, M. S. P. (2016). Electrophoretic deposition of graphene-related materials: a review of the fundamentals. *Prog. Mater. Sci.* 82, 83–117. doi: 10.1016/j.pmatsci.2016.03.002

Dimitrios, T., Nikos, T., Alberto, B., and Maurizio, P. (2006). Chemistry of carbon nanotubes. *Chem. Rev.* 106, 1105–1136. doi: 10.1021/cr050569o

Ding, J.-T., Meng, F.-T., Sui, J., and Meng, Z.-L. (2018). A review of graphene dispersion method. *Appl. Chem. Ind.* 47, 1043–1047. doi: 10.16581/j.cnki.issn1671-3206.20180330.043

Du, S. Y. (2007). Advanced composite materials and aerospace engineering. *Acta Mater. Composit. Sin.* 24, 1–12. doi: 10.3321/j.issn:1000-3851.2007.01.001

Ehli, C., Rahman, G. M. A., Jux, N., Balbinot, D., Guldi, D. M., Paolucci, F., et al. (2006). Interactions in single wall carbon nanotubes/pyrene/porphyrin nanohybrids. *J. Am. Chem. Soc.* 128, 11222–11231. doi: 10.1021/ja0624974

Fadavi, B. A., Tahamtan, S., Yazdani, S., Khosroshahi, R. A., Wei, D., Sahamirad, H., et al. (2016). Graphene tweaking Hamaker Constant of SiC nanoparticles: a new

horizon to solve the conflict between strengthening and toughening. *Scripta Mater*. 119, 65–69. doi: 10.1016/j.scriptamat.2016.02.028

Fu, C. L., and Yang, X. N. (2013). Molecular dynamics simulation of graphene exfoliation in water. *J. Nanjing Tech Univ. Nat. Sci. Ed.* 35, 87–90. doi: 10.3969/j.issn.1671-7627.2013.04.018

Gai, Y. Z., Wang, W. C., Xiao, D., and Zhao, Y. P. (2018). Ultrasound coupled with supercritical carbon dioxide for exfoliation of graphene: simulation and experiment. *Ultrason. Sonochem*. 41, 181–188. doi: 10.1016/j.ultsonch.2017.09.007

Gao, H. Y., Zhu, K. X., Hu, G. X., and Xue, C. (2017). Large-scale graphene production by ultrasound-assisted exfoliation of natural graphite in supercritical CO_2/H_2O medium. *Chem. Eng. J*. 308, 872–879. doi: 10.1016/j.cej.2016.09.132

Gao, Y., Cao, T. F., Cellini, F., Berger, C., de Heer, W. A., Tosatti, E., et al. (2018). Ultrahard carbon film from epitaxial two-layer graphene. *Nat. Nanotechnol.* 13, 133–138. doi: 10.1038/s41565-017-0023-9

Geng, H.-Z., Wang, J., Luo, Z. J., Da,S.-X., and Jia, S.-L. (2017). Graphene oxides-assisted dispersion of single-wall carbon nanotubes and conductivity of films. *J. Tianjin Polytech. Univ.* 36, 17–27. doi: 10.3969/j.issn.1671-024x.2017.06.004

Georgakilas, V., Otyepka, M., Bourlinos, A. B., Chandra, V., Kim, N., Kemp, K. C., et al. (2012). Functionalization of graphene: covalent and non-covalent approaches, derivatives and applications. *Chem. Rev*. 112, 6156–6214. doi: 10.1021/cr3000412

Georgakilas, V., Tiwari, J. N., Kemp, K. C., Perman, J. A., Bourlinos, A. B., Kim, K. S., et al. (2016). Noncovalent functionalization of graphene and graphene oxide for energy materials, biosensing, catalytic, and biomedical applications. *Chem. Rev*. 116, 5464–5519. doi: 10.1021/acs.chemrev.5b00620

Gou, X., Fu, Q., Tian, R., Gao, X.-D., Zhu, H.-L., and Li, H. (2016). Dynamic light scattering technology determination the Hamaker Constant of soil/clay colloid. *J. Southwest Univ. Nat. Sci. Ed*. 38, 74–81. doi: 10.13718/j.cnki.xdzk.2016.06.013

Green, A. A., and Hersam, M. C. (2010). Emerging methods for producing monodisperse graphene dispersions. *J. Phys. Chem. Lett.* 1, 544–549. doi: 10.1021/jz900235f

Gu, L., Ding, J. H., and Yu, H. B. (2016). Research in graphene-based anticorrosion coatings. *Prog. Chem*. 28, 737–743. doi: 10.7536/PC151109

Gu, L., Liu, S., Zhao, H. C., and Yu, H. B. (2015). Facile preparation of water-dispersible graphene sheets stabilized by carboxylated oligoanilines and their anticorrosion coatings. *ACS Appl. Mater. Interf.* 7, 17641–17648. doi: 10.1021/acsami.5b05531

Hadi, A., Zahirifar, J., Karimi-Sabet, J., and Dastbaz, A. (2018). Graphene nanosheets preparation using magnetic nanoparticle assisted liquid phase exfoliation of graphite: the coupled effect of ultrasound and wedging nanoparticles. *Ultrason. Sonochem*. 44, 204–214. doi: 10.1016/j.ultsonch.2018.02.028

Huang, B. Z. (2007). Microscopic mechanism and model design of close packing theory. *Pet. Drilling Tech*. 35, 5–12. doi: 10.3969/j.issn.1001-0890.2007.01.002

Huan-Yan, X., Bo, L., Tian-Nuo, S., Yuan, W., and Sridhar, K. (2018). Nanoparticles of magnetite anchored onto few-layer graphene: a highly efficient fenton-like nanocomposite catalyst. *J. Colloid Interf. Sci.* 532, 161–170. doi: 10.1016/j.jcis.2018.07.128

Israelachvili, J. N. (2011). Intermolecular and surface forces. *Q. Rev. Biol*. 2, 59–65. doi: 10.1016/0304-3991(92)90246-G

Ji, T., Tan, L. C., Bai, J. X., Hu, X. T., Xiao, S. Q., and Chen, Y. W. (2016). Synergistic dispersible graphene: sulfonated carbon nanotubes integrated with Pedot for large-scale transparent conductive electrodes. *Carbon* 98, 15–23. doi: 10.1016/j.carbon.2015.10.079

Jung, S. M., Mafra, D. L., Lin, C.-T., Jung, H. Y., and Kong, J. (2015). Controlled porous structures of graphene aerogels and their effect on supercapacitor performance. *Nanoscale* 7, 4386–4393. doi: 10.1039/C4NR07564A

Khan, U., O'Neill, A., Lotya, M., De, S., and Coleman, J. N. (2010). High concentration solvent-exfoliation of graphene. *Small* 6, 864–871. doi: 10.1002/smll.200902066

Kim, H., Abdala, A. A., and Macosko, C. W. (2010). Graphene/polymer nanocomposites. *Macromolecules* 43, 6515–6530. doi: 10.1021/ma100572e

Kozbial, A., Li, Z., Conaway, C., McGinley, R., Dhingra, S., Vahdat, V., et al. (2014). Study on the surface energy of graphene by contact angle measurements. *Langmuir* 30, 8598–8606. doi: 10.1021/la5018328

Laaksonen, P., Kainlauri, M., Laaksonen, T., Shchepetov, A., Jiang, H., Ahopelto, J., et al. (2010). Interfacial engineering by proteins: exfoliation and functionalization of graphene by hydrophobins. *Angew. Chem*. 122, 5066–5069. doi: 10.1002/ange.201001806

Lee, J. H., Avsar, A., Jung, J., Tan, J. Y., Watanabe, K., Taniguchi, T., et al. (2015). Van der waals force: a dominant factor for reactivity of graphene. *Nano Lett*. 15, 319–325. doi: 10.1021/nl5036012

León, V., Rodriguez, A. M., Prieto, P., Prato, M., and Vázquez, E. (2013). Exfoliation of graphite with triazine derivatives under ball-milling conditions: preparation of few-layer graphene via selective noncovalent interactions. *ACS Nano* 8, 563–571. doi: 10.1021/nn405148t

Li, B., Wang, T. K., Wang, X., Wu, X., Wang, C. Y., Miao, F., et al. (2019). Engineered recombinant proteins for aqueous ultrasonic exfoliation and dispersion of biofunctionalized 2D materials. *Chem-Eur. J*. 25, 7991–7997. doi: 10.1002/chem.201900716

Li, C., and Shi, G. Q. (2014). Functional gels based on chemically modified graphenes. *Adv. Mater*. 26, 3992–4012. doi: 10.1002/adma.201306104

Li, C., Xu, Y.-T., Zhao, B., Jiang, L., Chen, S.-G., Xu, J.-B., et al. (2016). Flexible graphene electrothermal films made from electrochemically exfoliated graphite. *J. Mate. Sci*. 51, 1043–1051. doi: 10.1007/s10853-015-9434-x

Li, D., Müller, M. B., Gilje, S., Kaner, R. B., and Wallace, G. G. (2008). Processable aqueous dispersions of graphene nanosheets. *Nat. Nanotechnol*. 3, 101–105. doi: 10.1038/nnano.2007.451

Li, J. T., Ye, F., Vaziri, S., Muhammed, M., Lemme, M. C., and Östling, M. (2012). A simple route towards high-concentration surfactant-free graphene dispersions. *Carbon* 50, 3113–3116. doi: 10.1016/j.carbon.2012.03.011

Li, Q., Lu, L. H., and Ding, A. J. (2017). Design of cleaning machine and cleaning effect research based on ultrasonic. *Phys. Exp. Coll.* 30, 31–35. doi: 10.14139/j.cnki.cn22-1228.2017.005.008

Li, Z., Bai, L., and Zheng, J. P. (2018). Effect of π-π interaction between carbon nanotubes and phenyl groups on the thermal stability of silicone rubber. *J. Therm. Anal. Calorim*. 131, 2503–2512. doi: 10.1007/s10973-017-6770-x

Lim, H. J., Lee, K., Cho, Y. S., Kim, Y. S., Kim, T., and Park, C. R. (2014). Experimental consideration of the Hansen solubility parameters of as-produced multi-walled carbon nanotubes by inverse gas chromatography. *Phys. Chem. Chem. Phys. PCCP*. 16, 17466–17472. doi: 10.1039/C4CP02319F

Liu, L. C., Zhou, M., Jin, L., Li, L. C., Mo, Y. T., Su, G. S., et al. (2019). Recent advances in friction and lubrication of graphene and other 2D materials: mechanisms and applications. *Friction* 7, 199–216. doi: 10.1007/s40544-019-0268-4

Liu, L. L., Zhou, M., Li, X., Jin, L., Su, G. S., Mo, Y. T., et al. (2018). Research progress in application of 2D materials in Liquid-phase lubrication system. *Materials* 11, 1314–1330. doi: 10.3390/ma11081314

Liu, W. W., Lei, H. I., Zhang, Y. C., Feng, L. J., Zheng, X. R., Li, B., et al. (2017). Research progress of biomolecule-assisted exfoliation and dispersion of graphene two-dimensional materials. *Eng. Plast. Appl.* 45, 120–123. doi: 10.3969/j.issn.1001-3539.2017.02.027

Liu, Y. J., Tai, Z. X., Zhang, J., Pang, W. K., Zhang, Q., Feng, H. F., et al. (2018). Boosting potassium-ion batteries by few-layered composite anodes prepared via solution-triggered one-step shear exfoliation. *Nat. Commun.* 9:3654. doi: 10.1038/s41467-018-05786-1

Long, X. J., Li, B., Wang, L., Huang, J. Y., Zhu, J., and Lou, S. N. (2016). Shock response of Cu/graphene nanolayered composites. *Carbon* 103, 457–463. doi: 10.1016/j.carbon.2016.03.039

Luo, Y. X., Gao, X. D., Tian, R., and Li, H. (2018). Approach to estimation of Hamaker Constant as taking hofmeister effects into account. *J. Phys. Chem. C* 122, 9432–9440. doi: 10.1021/acs.jpcc.7b12830

Mao, J. J., Iocozzia, J., Huang, J. Y., Meng, K., Lai, Y. K., and Lin, Z. Q. (2018). Graphene aerogels for efficient energy storage and cconversion. *Energy Environ. Sci.* 11, 772–799. doi: 10.1039/C7EE03031B

Melios, C., Giusca, C. E., Panchal, V., and Kazakova, O. (2018). Water on graphene: review of recent progress. *2D Mater.* 5:22001. doi: 10.1088/2053-1583/aa9ea9

Meuer, S., Braun, L., and Zentel, R. (2009). Pyrene containing polymers for the non-covalent functionalization of carbon nanotubes. *Macromol. Chem. Phys.* 210, 1528–1537. doi: 10.1002/macp.200900125

Moorthy, I. G., Maran, J. P., Surya, S. M., Naganyashree, S., and Shivamathi, C. S. (2015). Response surface optimization of ultrasound assisted extraction

of pectin from pomegranate peel. *Int. J. Biol. Macromol.* 72, 1323–13285. doi: 10.1016/j.ijbiomac.2014.10.037

Munuera, M. J., Paredes, J. I., Villar-Rodil, S., Ayán-Varela, M., Pagán, A., Aznar-Cervantes, S. D., et al. (2016). High quality, low oxygen content and biocompatible graphene nanosheets obtained by anodic exfoliation of different graphite types. *Carbon* 94, 729–739. doi: 10.1016/j.carbon.2015.07.053

Narayan, R., Lim, J., Jeon, T., Li, D. J., and Kim, S. O. (2017). Perylene tetracarboxylate surfactant assisted liquid phase exfoliation of graphite into graphene nanosheets with facile re-dispersibility in aqueous/organic polar solvents. *Carbon* 119, 555–568. doi: 10.1016/j.carbon.2017.04.071

Nduwimana, A., and Wang, X.-Q. (2009). Energy gaps in supramolecular eunctionalized graphene nanoribbons. *ACS Nano* 3, 1995–1999. doi: 10.1021/nn9004268

Notley, S. M. (2012). Highly concentrated aqueous suspensions of graphene through ultrasonic exfoliation with continuous surfactant addition. *Langmuir* 28, 14110–14113. doi: 10.1021/la302750e

Novoselov, K. S., Geim, A. K., Morozov, S. V., Jiang, D., Zhang, Y., Dubonos, S. V., et al. (2004). Electric field effect in atomically thin carbon films. *Science* 306, 666–669. doi: 10.1126/science.1102896

O'Neill, A., Khan, U., Nirmalraj, P. N., Boland, J., and Coleman, J. N. (2011). Graphene dispersion and exfoliation in low boiling point solvents. *J. Phys. Chem. C*. 115:13. doi: 10.1021/jp110942e

Paredes, J. I., and Villar-Rodil, S. (2016). Biomolecule-assisted exfoliation and dispersion of graphene and other two-dimensional materials: a review of recent progress and applications. *Nanoscale* 8, 15389–15413. doi: 10.1039/C6NR02039A

Park, S. J., An, J. H., Jung, I., Piner, R. D., An, S. J., Li, X. S., et al. (2009). Colloidal suspensions of highly reduced graphene oxide in a wide variety of organic solvents. *Nano Lett*. 9, 1593–1597. doi: 10.1021/nl803798y

Parvez, K., Wu, Z.-S., Li, R. J., Liu, X. J., Graf, R., Feng, X. L., et al. (2014). Exfoliation of graphite into graphene in aqueous solutions of inorganic salts. *J. Am. Chem. Soc.* 136, 6083–6091. doi: 10.1021/ja5017156

Parviz, D., Das, S., Ahmed, H. S. T., Irin, F., Bhattacharia, S., and Green, M. J. (2012). Dispersions of non-covalently functionalized graphene with minimal stabilizer. *ACS Nano* 6, 8857–8867. doi: 10.1021/nn302784m

Paton, K. R., Eswaraiah, V., Claudia, B., Smith, R. J., Umar, K., Arlene, O., et al. (2014). Scalable production of large quantities of defect-free few-layer graphene by shear exfoliation in liquids. *Nat. Mater.* 13, 624–630. doi: 10.1038/nmat3944

Phiri, J., Gane, P., and Maloney, T. C. (2017). High-concentration shear-exfoliated colloidal dispersion of surfactant–polymer-stabilized few-layer graphene sheets. *J. Mater. Sci.* 52, 8321–8337. doi: 10.1007/s10853-017-1049-y

Ping, Y. J., Gong, Y. N., and Pan, C. X. (2017). Research progress in preparation of graphene from electrochemical exfoliation and its optoelectronic characteristics. *Chin. J. Lasers.* 44, 104–119. doi: 10.3788/CJL201744.0703007

Qin, W. W., Li, Y., Teng, Y. Q., and Qin, T. (2018). Hydrogen bond-assisted synthesis of MoS_2/reduced graphene oxide composite with excellent electrochemical performances for lithium and sodium storage. *J. Colloid Interf. Sci.* 512, 826–833. doi: 10.1016/j.jcis.2017.10.106

Río, F. D., Boado, M. G., Rama, A., and Guitián, F. (2017). A comparative study on different aqueous-phase graphite exfoliation methods for few-layer graphene production and its application in alumina matrix composites. *J. Eur. Ceram. Soc.* 37, 3681–3693. doi: 10.1016/j.jeurceramsoc.2017.04.029

Rodriguez-Laguna, M. R., Castro-Alvarez, A., Sledzinska, M., Maire, J., Costanzo, F., Ensing, B., et al. (2018). Mechanisms behind the enhancement of thermal properties of graphene nanofluids. *Nanoscale* 10, 15402–15409. doi: 10.1039/C8NR02762E

Sadasivuni, K. K., Ponnamma, D., Thomas, S., and Grohens, Y. (2014). Evolution from graphite to graphene elastomer composites. *Prog. Polym. Sci.* 39, 749–780. doi: 10.1016/j.progpolymsci.2013.08.003

Sahoo, M., and Ramaprabhu, S. (2017). Solar synthesized tin oxide nanoparticles dispersed on graphene wrapped carbon nanotubes as a Li ion battery anode material with improved stability. *RSC Adv.* 7, 13789–13797. doi: 10.1039/C6RA27515J

Secor, E. B., Prabhumirashi, P. L., Puntambekar, K., Geier, M. L., and Hersam, M. C. (2013). Inkjet printing of high conductivity, flexible graphene patterns. *J. Phys. Chem. Lett.* 4, 1347–1351. doi: 10.1021/jz400644c

Selvakumar, N., Biswas, A., Krupanidhi, S. B., and Barshilia, H. C. (2018). Enhanced optical absorption of graphene-based heat mirror with tunable spectral selectivity. *Sol. Energ. Mat. Sol. C.* 186, 149–153.doi: 10.1016/j.solmat.2018.06

Seo, J.-W. T., Green, A. A., Antaris, A. L., and Hersam, M. C. (2011). High concentration aqueous dispersions of graphene using nonionic, biocompatible block copolymers. *J. Phys. Chem. Lett.* 2, 1004–1008. doi: 10.1021/jz2003556

Shabafrooz, V., Bandla, S., and Hanan, J. C. (2018). Graphene dispersion in a surfactant-free, polar solvent. *J. Mater. Sci.* 53, 559–572. doi: 10.1007/s10853-017-1456-0

Shao, J.-J., Lv, W., and Yang, Q.-H. (2014). Self-assembly of graphene oxide at interfaces. *Adv. Mater.* 26, 5586–5612. doi: 10.1002/adma.201400267

Shi, P. C., Guo, J. P., Liang, X., Cheng, S., Zheng, H., Wang, Y., et al. (2018). Large-scale production of high-quality graphene sheets by a non-electrified electrochemical exfoliation method. *Carbon* 126, 507–513. doi: 10.1016/j.carbon.2017.10.071

Shinde, D. B., Brenker, J., Easton, C. D., Tabor, R. F., Neild, A., and Majunider, M. (2016). Shear assisted electrochemical exfoliation of graphite to graphene. *Langmuir* 32, 3552–3559. doi: 10.1021/acs.langmuir.5b04209

Si, Y. C., and Samulski, E. T. (2008). Synthesis of water soluble graphene. *Nano Lett.* 8, 1679–1682. doi: 10.1021/nl080604h

Song, S. H., Park, K. H., Kim, B. H., Choi, Y. W., Jun, G. H., Lee, D. J., et al. (2013). Enhanced thermal conductivity of epoxy-graphene composites by using non-oxidized graphene flakes with non-covalent functionalization. *Adv. Mater.* 23, 732–737. doi: 10.1002/adma.201202736

Su, C.-Y., Lu, A.-Y., Xu, Y. P., Chen, F.-R., Khlobystov, A. N., and Li, L.-J. (2011). High-quality thin graphene films from fast electrochemical exfoliation. *ACS Nano*. 5, 2332–2339. doi: 10.1021/nn200025p

Tang, L. H., Wang, Y., Li, Y. M., Feng, H. B., Lu, J., and Li, J. H. (2009). Preparation, structure, and electrochemical properties of reduced graphene sheet films. *Adv. Funct. Mater.* 19, 2782–2789. doi: 10.1002/adfm.200900377

Tang, Z., Tang, C. H., and Gong, H. (2014). A high energy density asymmetric supercapacitor from nano-architectured $Ni(OH)_2$/carbon nanotube electrodes. *Adv. Funct. Mater.* 22, 1272–1278. doi: 10.1002/adfm.201102796

Tchernook, A., Krumova, M., Tölle, F. J., Mülhaupt, R., and Mecking, S. (2014). Composites from aqueous polyethylene nanocrystal/graphene dispersions. *Macromolecule* 47, 3017–3021. doi: 10.1021/ma500394r

Tian, J., Guo, L., Shen, S., Zhang, Y., Yin, X. L., and Wu, W. (2017). Research progress on preparation of graphene by liquid exfoliation method. *China Powder Sci. Technol.* 23, 45–49. doi: 10.13723/j.issn.1008-5548.2017.03.009

Tian, L. L., Anilkumar, P., Cao, L., Kong, C. Y., Meziani, M. J., Qian, H. J., et al. (2011). Graphene oxides dispersing and hosting graphene sheets for unique nanocomposite materials. *ACS Nano* 5, 352–358. doi: 10.1021/nn200162z

Tkalya, E. E., Ghislandi, M., de With, G., and Koning, C. E. (2012). The use of surfactants for dispersing carbon nanotubes and graphene to make conductive nanocomposites. *Curr. Opin. Collpid In.* 17, 225–232. doi: 10.1016/j.cocis.2012.03.001

Tour, J. M. (2014). Scaling up exfoliation. *Nat. Mater.* 13, 545–546. doi: 10.1038/nmat3961

Tung, T. T., Yoo, J., Alotaibi, F. K., Nine, M. J., Karunagaran, R., Krebsz, M., et al. (2016). Graphene oxide-assisted liquid phase exfoliation of graphite into graphene for highly conductive film and electromechanical sensors. *ACS Appl. Mater. Interfaces* 8, 16521–16532. doi: 10.1021/acsami.6b04872

Uchaker, E., and Cao, G. Z. (2014). Mesocrystals as electrode materials for lithium-ion batteries. *Nano Today* 9, 499–524. doi: 10.1016/j.nantod.2014.06.004

Vadukumpully, S., Paul, J., Mahanta, N., and Valiyaveettil, S. (2011). Flexible conductive graphene/poly(vinyl chloride) composite thin films with high mechanical strength and thermal stability. *Carbon* 49, 198–205. doi: 10.1016/j.carbon.2010.09.004

Vallés, C., Drummond, C., Saadaoui, H., Furtado, C. A., He, M. S., Roubeau, O., et al. (2008). Solutions of negatively charged graphene sheets and ribbons. *J. Am. Chem. Soc.* 130, 15802–15804. doi: 10.1021/ja808001a

Vashist, S. K., and Luong, J. H. T. (2015). Recent advances in electrochemical biosensing schemes using graphene and graphene-based nanocomposites. *Carbon* 84, 519–550. doi: 10.1016/j.carbon.2014.12.052

Wan, Y.-J., Tang, L.-C., Yan, D., Zhao, L., Li, Y.-B., Wu, L.-B., et al. (2013). Improved dispersion and interface in the graphene/epoxy composites via a facile surfactant-assisted process. *Compos. Sci. Technol.* 82, 60–68. doi: 10.1016/j.compscitech.2013.04.009

Wang, H., Zhang, J. H., and Zhao, Y.-F. (2018). Research progress on graphene/polymer composites with non-covalent surface modification. *J. Mater Eng*. 46, 44–52. doi: 10.11868/j.issn.1001-4381.2016.000011

Wang, J., and Chen, B. L. (2015). Adsorption and coadsorption of organic pollutants and a heavy metal by graphene oxide and reduced graphene materials. *Chem. Eng. J*. 281, 379–388. doi: 10.1016/j.cej.2015.06.102

Wang, Q. H., Wang, X. J., and Fang, J. J. (2016). Application of graphene in epoxy zinc rich primer. *Paint Coat. Ind*. 46, 42–47. doi: 10.3969/j.issn.0253-4312.2016.12.007

Wang, S. F., Wang, C., Ji, X., and Lin, M. Z. (2018). Surfactant- and sonication- free exfoliation approach to aqueous graphene dispersion. *Mater. Lett*. 217, 67–70. doi: 10.1016/j.matlet.2018.01.064

Wang, W. Z., Zhang, Y., and Wang, Y.-B. (2014). Noncovalent $\pi \cdots \pi$ interaction between graphene and aromatic molecule: structure, energy, and nature. *J. Chem. Phys*. 140, 094302–094308. doi: 10.1063/1.4867071

Wang, X. D., Liu, X. H., Yuan, H. Y., Liu, H., Liu, C. T., Li, T. X., et al. (2018). Non-covalently functionalized graphene strengthened poly(vinyl alcohol). *Mater. Design*. 139, 372–379. doi: 10.1016/j.matdes.2017.11.023

Wang, X. J., Xu, R.-X., Dun, T., Qi, K.-C., Cao, G.-C., and Lin, Z.-L. (2017). Study on preparation and properties of the graphene functional layer by the spray coating method. *J. Univ. Electron. Sci. Technol. China* 46, 151–155. doi: 10.3969/j.issn.1001-0548.2017.01.020

Wegst, U. G. K., Bai, H., Saiz, E., Tomsia, A. P., and Ritchie, R. O. (2015). Bioinspired structural materials. *Nat. Mater*. 14, 23–36. doi: 10.1038/nmat4089

Wei, W., Lv, W., and Yang, G. H. (2011). High-concentration graphene aqueous suspension and a membrane self-assembled at the liquid-air interface. *New Carbon Mater*. 26, 36–40. doi: 10.1016/j.carbon.2011.02.037

Xia, K. L., Wang, C. Y., Jian, M. Q., Wang, Q., and Zhang, Y. Y. (2018). CVD growth of fingerprint-like patterned 3D graphene film for an ultrasensitive pressure sensor. *Nano Res*. 11, 1124–1134. doi: 10.1007/s12274-017-1731-z

Xie, J.-L., Chen, X.-Y., Huang, J., Liu, Z.-R., and Li, H. (2014). Synthesis and characterization of stable graphene colloidal dispersion. *J. Funct. Mater*. 45, 12108–12112. doi: 10.3969/j.issn.1001-9731.2014.12.021

Xu, M. L., He, X. F., He, C. F., Fan, L. D., and Li, J. F. (2016). Research progress in graphene/polymer composites. *Chain Plast. Ind*. 44, 27–33. doi: 10.3969/j.issn.1005-5770.2016.02.007

Xu, X. J., Qin, J. G., and Li, Z. (2009). Research advances of graphene. *Prog. Chem*. 21, 2559–2567. doi: 10.1016/S1874-8651(10)60079-8

Xu, Z., Lei, X. L., Tu, Y. S., Tan, Z.-J., Song, B., and Fang, H. P. (2017). Dynamic cooperation of hydrogen binding and π stacking in ssDNA adsorption on graphene oxide. *Chem-Eur. J*. 23, 13100–11304. doi: 10.1002/chem.201701733

Yang, J., Yang, X. N., and Li, Y. P. (2015). Molecular simulation perspective of liquid-phase exfoliation, dispersion, and stabilization for graphene. *Curr. Opin. Colloid In*. 20, 339–345. doi: 10.1016/j.cocis.2015.10.005

Yang, K., Zhang, S., Zhang, G. X., Sun, X. M., Lee, S.-,Tong., and Liu, Z. (2010). Graphene in mice: ultrahigh *in vivo* tumor uptake and efficient photothermal therapy. *Nano Lett*. 9, 3318–3323. doi: 10.1021/nl100996u

Yang, Q., and Yang, J. H. (2018). Preparation and application of graphene dispersion with high concentration. *New Chem. Mater*. 46, 253–256. doi: 10.1021/jp1037443

Yang, X. M., Li, L., Shang, S. M., and Tao, X.-M. (2010). Synthesis and characterization of layer-aligned poly(vinyl alcohol)/graphene nanocomposites. *Polymer* 51, 3431–3435. doi: 10.1016/j.polymer.2010.05.034

Yi, M., and Shen, Z. G. (2015). A review on mechanical exfoliation for scalable production of graphene. *J. Mater. Chem. A* 3, 11700–11715. doi: 10.1039/C5TA00252D

Yi, M., Shen, Z. G., Zhang, X. J., and Ma, S. L. (2013). Achieving concentrated graphene dispersions in water/acetone mixtures by the strategy of tailoring Hansen solubility parameters. *J. Phys. D. Appl. Phys*. 46:025301. doi: 10.1088/0022-3727/46/2/025301

Yoon, W., Lee, Y., Jang, H., Jang, M., Kim, J. S., Lee, H. S., et al. (2015). Graphene nanoribbons formed by a sonochemical graphene unzipping using flavin mononucleotide as a template. *Carbon* 81, 629-638. doi: 10.1016/j.carbon.2014.09.097

Yu, P. C., Fesenko, V. I., and Tuz, V. R. (2018). Dispersion features of complex waves in a graphene-coated semiconductor nanowire. *Nanophotonics* 7, 925–934. doi: 10.1515/nanoph-2018-0026

Yue, L., Pircheraghi, G., Monemian, S. A., and Manas-Zloczower, I. (2014). Epoxy composites with carbon nanotubes and graphene nanoplatelets-dispersion and synergy effects. *Carbon* 78, 268–278. doi: 10.1016/j.carbon.2014.07.003

Zhang, J. (2016). *Rational Design of a Graphene Dispersant*. Manchester: ProQuest Dissertations Publishing.

Zhang, J., Xu, L., Zhou, B., Zhu, Y., and Jiang, X. (2017). The pristine graphene produced by liquid exfoliation of graphite in mixed solvent and its application to determination of dopamine. *J Colloid Interf. Sci*. 513, 279–286. doi: 10.1016/j.jcis.2017.11.038

Zhang, L. (2018). Applications and research progress of graphene materials. *Educ. Modern*. 5, 275–278.

Zhang, Q. C., and Huang, S. P. (2000). Prospect of dispersant's application in aoueous systems. *China Powder Sci. Technol*. 6, 32–35. doi: 10.3969/j.issn.1008-5548.2000.04.009

Zhang, X. Q., Tang, Y. J., Wang, X. Y., Zhang, J. H., Guo, D. L., and Zhang, X. M. (2018). Dispersion and rheological properties of aqueous graphene suspensions in presence of nanocrystalline cellulose. *J. Polym. Environ*. 26, 3502–3510. doi: 10.1007/s10924-018-1237-0

Zhang, Y. B., Tang, T.-T., Girit, C., Hao, Z., Martin, M. C., Zettl, A., et al. (2009). Direct observation of a widely tunable bandgap in bilayer graphene. *Nature* 459, 820–823. doi: 10.1038/nature08105

Zhang, Z. X., Huang, H. L., Yang, X. M., and Zang, L. (2011). Tailoring electronic properties of graphene by π-π stacking with aromatic molecules. *J. Phys. Chem. Lett*. 2, 2897–2905. doi: 10.1021/jz201273r

Zhao, D. M., Li, Z. W., Liu, L. D., Zhang, Y. H., Ren, D., and Li, J.ian. (2014). Progress of preparation and application of graphene/carbon nanotube composite materials. *Acta Chim. Sin*. 2, 185–200. doi: 10.6023/A13080857

Zhao, H. L., Cai, W. H., Wang, L., Yu, J. Y., and Wang, L. K. (2018). Study on dispersion stability of graphene in surfactants aqueous solutions. *J. Yanshan Univ*. 42, 377–385. doi: 10.3969/j.issn.1007-791X.2018.05.001

Zhao, S. H., Chen, Y., Wang, S. L., Rao, Y. C., and Shi, X. J. (2017). Research progress in anti-corrosion coatings containing graphene. *J. Changzhou Univ. Natl. Sci. Ed*. 29, 23–28. doi: 10.3969/j.issn.2095-0411.2017.02.005

Zhao, X. J., Tao, L. M., Li, H., Huang, W. C., Sun, P. Y., Liu, J., et al. (2018). Efficient planar perovskite solar cells with improved fill factor via interface engineering with graphene. *Nano Lett*. 18, 2442–2449. doi: 10.1021/acs.nanolett.8b00025

Zhou, P.-P., and Zhang, R.-Q. (2015). Physisorption of benzene derivatives on graphene: critical roles of steric and stereoelectronic effects of the substituent. *Phys. Chem. Chem. Phys*. 17, 12185–12193. doi: 10.1039/C4CP05973E

Zhou, S. Q., Lamperski, S., and Sokołowska, M. (2017). Classical density functional theory and monte carlo simulation study of electric double layer in the vicinity of a cylindrical electrode. *J. Stat. Mech-Theory E*. 2017:73207. doi: 10.1088/1742-5468/aa79af

Zhu, L. X., Zhao, X., Li, Y. Z., Yu, X. Y., Li, C., and Zhang, Q. H. (2013). High-quality production of graphene by liquid-phase exfoliation of expanded graphite. *Mater. Chem. Phys*.137, 984–990. doi: 10.1016/j.matchemphys.2012.11.012

Zhu, Y. Q., Wang, F. Y. K., Zhang, C., and Du, J. Z. (2014). Preparation and mechanism insight of nuclear envelope-like polymer vesicles for facile loading of biomacromolecules and enhanced biocatalytic activity. *ACS Nano* 8, 6644–6654. doi: 10.1021/nn502386j

Zou, P., Shi, W.-R., Yang, S.-H., and Huang, D.-H. (2014). Preparation of graphene by chemical vapor deposition. *J. Mater. Sci. Eng*. 32, 264–267. doi: 10.1016/j.carbon.2011.02.043

Conflict of Interest: The authors declare that the research was conducted in the absence of any commercial or financial relationships that could be construed as a potential conflict of interest.